

Pavol Jozef Šafárik University in Košice



SPRING ELECTROCHEMICAL MEETING

BOOK OF ABSTRACTS

March 17.-18.2022, Košice, Slovakia

Ivana Šišoláková (ed.)

Košice 2022

Edited by:

RNDr. Ivana Šišoláková, PhD.,

Pavol Jozef Šafárik University in Košice, ivana.sisolakova@upjs.sk

Reviewed by:

prof. RNDr. Renáta Oriňaková, DrSc.,

Pavol Jozef Šafárik University in Košice, renata.orinakova@upjs.sk

doc. RNDr. Andrea Straková Fedorková, PhD.,

Pavol Jozef Šafárik University in Košice, andrea.fedorkova@upjs.sk

Scientific Committee:

Prof. Renáta Oriňaková, UPJS Kosice

Dr. Jana Shepa, UPJS Kosice

Dr. Radka Gorejová, UPJS Kosice

Dr. Ivana Šišoláková, UPJS Kosice

Organisation Committee:

RNDr. Ivana Šišoláková, PhD.

RNDr. Radka Gorejová

RNDr. Jana Shepa

RNDr. Dominika Capková

This work is licensed under a Creative Commons 4.0 - CC BY NC ND
Creative Commons Attribution –NonCommercial - No-derivates 4.0



The authors are responsible for the content of this publication.

Available at: www.unibook.upjs.sk

Publication date: 05.04.2022

ISBN 978-80-574-0089-9 (e-publication)

LIST OF CONTENTS

Preface.....	5
Chronopotentiometric Antioxidant Measuring Method with Improved Measuring Properties.....	6
Elimination Voltammetry with Linear Scan as an Innovative Tool for	9
Electroanalysis of Biomolecules	9
MOF-76(Gd) as an Effective Humidity Sensor Detected by Resistance.....	12
Hydrogen Storage and Humidity Sensing Using MOF-76(Tb).....	15
Mesoporous Material MIL-101 as an Additive in LiS Batteries	18
Effect of MOF-76(Gd) Activation/Carbonization on the Cycle Performance Stability in Li-S Battery	21
Sr(II) and Ba(II) Alkaline Earth Metal-Organic Frameworks (AE-MOFs) as Materials for Energy Storage and Selective Gas Adsorption	22
Electrochemical oxidation of industrial pollutants in groundwater from landfill of chemical waste disposal site CHZJD Bratislava-Vrakuňa	25
Study of stability of molybdenum-nickel electrocatalyst for hydrogen evolution reaction in alkaline solution	29
Infiltration of Sulphur into a Porous Conductive Host Based on a Metal-Organic Framework and its Application as a Cathode in Li-S Batteries.....	31
Voltammetric determination of ciprofloxacin in the flow system using a boron-doped diamond electrode.....	34
Electrochemical Deposition of Hydroxyapatite Coatings on the Zinc-based Substrates	37
Effect of thickness of NiCoP doped carbon fiber layers on their catalytic activity towards hydrogen evolution reaction	39
Analytical characteristics of screen-printed carbon electrode modified by polypyrrole and NiO nanoparticles as a sensor for insulin determination	42
PSM of Microporous Gallium-Porphyrin Frameworks for Gas Adsorption and Energy Storage in Li-S Batteries	44
Boronic Acids and Ferrocenes – from Electroactive Molecular Probes to ROS-activated Prodrugs.....	47
Microscopic Simulation of Li-ion Battery.....	50
Activated carbon as a conductive host in Li-S battery	53

Nickel nanocavity prepared by colloidal lithography as a suitable electrochemical sensor for insuline detection	55
Metal-organic frameworks containing fluorinated ligands.....	56
Electrochemical Determination of Insulin	58
SBA-15 coated with nanocrystalline NiO-doped anatase as heterogeneous catalyst for photodegradation of organic molecules.....	60

Preface

On behalf of the **Spring Electrochemical Meeting** Organizing Committees, we introduce with pleasure these proceedings devoted to contributions from **Spring Electrochemical Meeting** held in Košice, Slovakia. The conference is organized by the **Faculty of Science Pavol Jozef Šafárik University in Košice** and **Czechoslovak Student Chapter** sponsored by **Visegradfund project number 22020140**. The conference program provides an opportunity for researchers interested in electrochemistry to discuss their latest results and exchange ideas on the new trends. The main objective of the conference umbrella is to encourage discussion on a broad range of related topics and to stimulate new collaborations among the participants. We hope that these proceedings will give readers an excellent overview of important and diversity topics discussed at the conference. We thank all authors for submitting their latest work, thus contributing to the excellent technical contents of the Conference. Especially, we would like to thank the organizers that worked diligently to make this conference a success, and to the recenzents for the thorough and careful review of the papers. We wish all attendees of Spring Electrochemical Meeting 2022 an enjoyable scientific gathering in Košice, Slovakia. I wish all participants enjoy this scientific meeting to collect new information form electrochemistry.

.....

Ivana Šišoláková

Invited Lecture

Chronopotentiometric Antioxidant Measuring Method with Improved Measuring Properties

Lawrence K. Muthuri^{a*}, Livia.Nagy^{a, b}, Geza.Nagy^{a, b}

^a Department of Physical Chemistry and Materials Science, Faculty of Sciences, University of Pécs, 7624, Ifjúság u. 6 Pécs, Hungary

^b Szentágothai J. Research Center, University of Pécs, 7624, Ifjúság u. 20, Pécs, Hungary

*lkm79@gmail.com

Recently we proposed a novel method for determining antioxidant activity in various samples [1]. It employed glassy carbon working electrode (GCE) chemically modified with a thin immobilized redox mediator film on its surface. A two-step protocol was followed during measurement. Initially, a short (1-2 s) controlled potential step brought the film to its oxidized state. In the second step, the potential control was disconnected, and the open cell potential (OCP) of the electrode was followed in time. Exposure of the oxidized film to an antioxidant containing media causes a redox potential change. By evaluating the initial slope of the electrode potential – time function, the antioxidant activity of a sample could be assessed. The method employed Meldola Blue (MB), (N,N dimethyl-7-amino-1,2-benzophenoxazinium ion) mediator layer immobilized on the electrode surface. L-ascorbic acid as antioxidant analyte was used.

In our latest work, electrochemically prepared reduced graphene oxide (GO) linker film was used to increase stability and activity of the MB redox layer. Furthermore the applicability of the method for measuring different antioxidants has been tested. In the Conference our most recent results obtained with the application of the novel chronopotentiometric method will be presented.

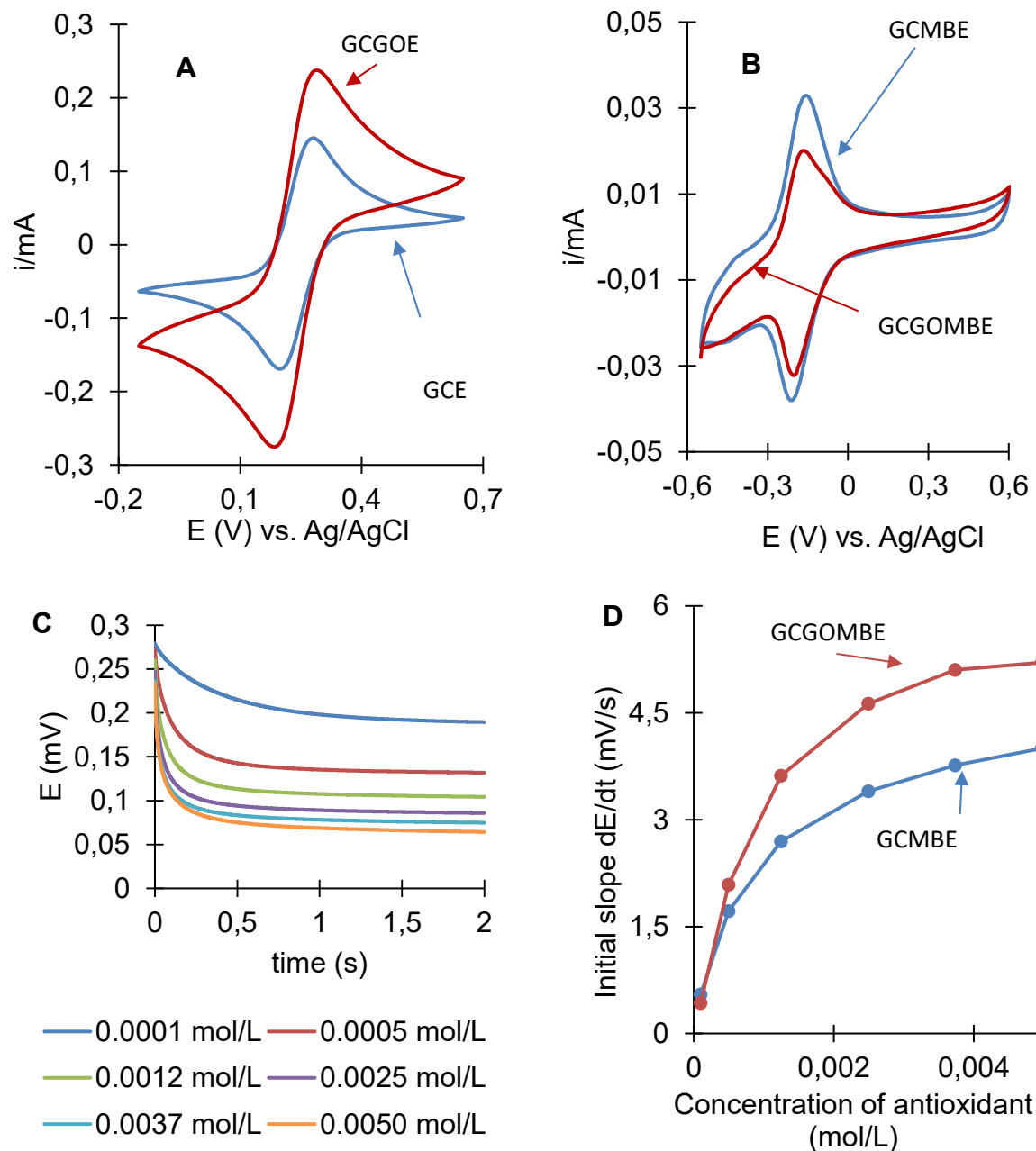


Figure 1: (A) Cyclic voltammograms (CVs) recorded in 0.5M KCl solution containing 5 mM $K_4(Fe(CN)_6)$ with electrochemically pre-treated glassy carbon electrode with no GO layer (GCE), with graphene oxide layer (GCGOE) Scanning rate 50 mV/s. (B) CVs of GCE modified with MB and GCGOE modified with MB in 0.25M phosphate buffer solution pH 7, scan rate 50mV/s. (c) Chronopotentiometric relaxation curves of potential change over time for 0.0001mol/L to 0.005mol/L L-ascorbic acid antioxidant concentration. (D) Calibration plot of chronopotentiometric measurements for initial slope of potential-time function (dE/dt) against the concentration of L-ascorbic acid antioxidant.

Modification of the GCE with a GO linker layer indicates some improvement in the stability and sensitivity of adsorbed MB layer in chronopotentiometric measurements at OCP as well as repeatability of results.

Acknowledgements

Supported by the Visegrad Fund project number 22020140, NKFIH grant number K 125244 and academic sponsorship for Lawrence Kinyua Muthuri through the Stipendium Hungaricum scholarship program.

Reference

- [1] L.K. Muthuri, L. Nagy, G. Nagy, *Electrochem. Commun.* **122** (2021), 106907.

Elimination Voltammetry with Linear Scan as an Innovative Tool for Electroanalysis of Biomolecules

L. Trnkova

Department of Chemistry, Faculty of Science, Masaryk University, Kamenice 5, CZ-625
00 Brno, Czech Republic libuse@chemi.muni.cz

Elimination voltammetry with linear scan (EVLS) is a software method that transforms the total current-voltage records into elimination functions providing new useful information about electrode processes.

The EVLS procedure works based on different dependence of partial currents (e.g., diffusion, kinetic, and capacitive current components) on the polarization rate (scan rate v) (Fig.1). It combines total voltammetric currents measured at different scan rates into elimination functions, eliminating some partial currents and conserving others.

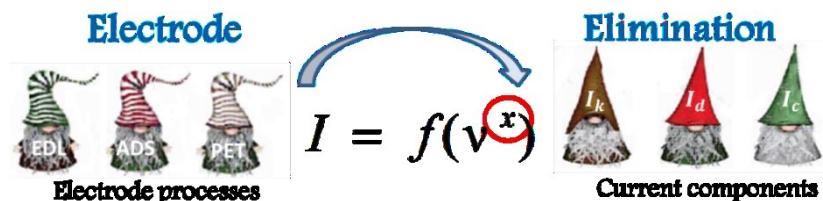


Figure 1: The graphical abstract of EVLS (EDL – Electrode double layer, ADS – adsorption, PET – Proton-electron transfer). The exponent x : $\frac{1}{2}$ for the diffusion current (I_d); $x=0$ for the kinetic current (I_k); and $x=1$ for the charging current (I_c).

For electroanalytical and mechanistic purposes, the EVLS E4 function, which eliminates charging and kinetic current components and conserves the diffuse current component, found the most useful application (Fig 2.). This elimination function became the indicator of the adsorption of electroactive particles because the EVLS E4 of adsorbed depolarizer results in the special peak-to-peak signal providing both better voltammetric sensitivity and better separation of overlapped signals.

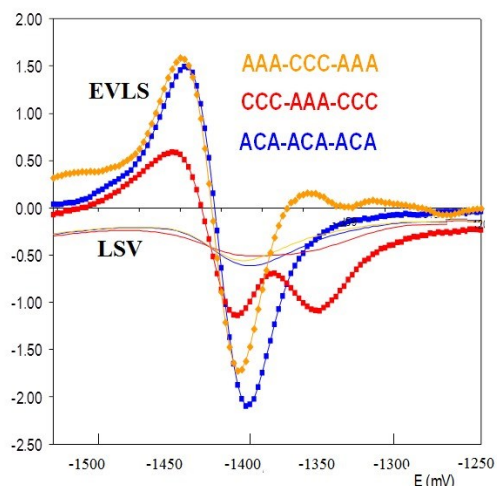


Figure 2: LSV and EVLS of nucleic acid nonamers (2 μM) with different positions of adenine (A) and cytosine (C). Common reduction signals of A and C were studied on a mercury electrode in the phosphate buffer (pH 6.4). The nonamers were adsorbed on the electrode surface at -100 mV for 120 s.

Based on a comparison of EVLS theoretical and experimental results, the elimination procedure achieves improvements and extensions in its applications (Fig.3).

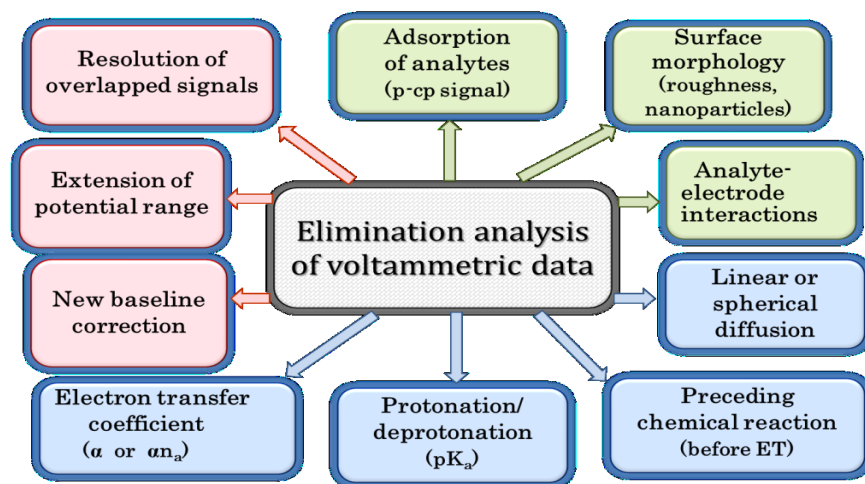


Figure 3: A diagram of EVLS applications in three analytical fields: The red segments represent the contribution of EVLS to increasing the sensitivity of voltammetric methods and enhancing the separation ability of LSV and CV signals. The green rectangles expose the possibility of using EVLS analysis to investigate phenomena affected by the morphology of the working electrode surface. The blue items represent assistance in the study of the electrode process mechanisms.

In the lecture, the advantages and disadvantages of EVLS applications will be discussed.

Acknowledgments

The research was supported by Masaryk University (MUNI/A/1192/2020 and MUNI/A/1539/2021) and the International Visegrad Fund (22020140).

References

- [1] O. Dracka, J. Electroanal. Chem. **402** (1996) 19-28.
- [2] L. Trnkova, J. Electroanal. Chem. **582** (2005) 258-266.
- [3] L. Trnkova, Application of EVLS in Bioelectrochemistry; in: Utilizing of BioElectrochemical and Mathematical Methods in Biological Research, Vol. 4. (Adam V. and Kizek R. eds.). Research Signpost, Kerala, India 2007, page 52.
- [4] L. Trnkova, J Electroanal. Chem. **905** (2022)115961.

Open session

MOF-76(Gd) as an Effective Humidity Sensor Detected by Resistance

A. Garg^a, R. Saini^b, A. Sharma^c, M. Alması^{d*}

^a Department of Physics, Suresh Gyan Vihar University, Jaipur 302017 India

^b Department of Physics and Astrophysics, School of Basic Sciences, Central University of Haryana, Mahendergarh 123031 India

^c Department of Physics, School of Engineering & Technology, Central University of Haryana, Mahendergarh 123031 India

^d Department of Inorganic Chemistry, Faculty of Science, P. J. Safarik University, Moyzesova 11, Kosice 041 54 Slovak Republic

*miroslav.almasi@upjs.sk

Numerous extents such as package food, biology, meteorology, agriculture, research labs and drug storage require controlled humidity. For distinguishing unstable substances at ppm-level concentrations, lots of humidity sensors are available in the market, but the challenge is with humidity sensing beneath ~100 ppm (few percentages relative humidity (RH) at 298 K). In many applications such as medicinal provisions, gas and fuel storage, agricultural products storage, semiconductor manufacturing, humidity sensing is obligatory at ppm or ppb level. There is a lot of research work published for humidity sensing, but humidity sensing at ppb level is a challenge. Manufacturing of humidity sensors having 90%RH is generally expensive. Even polymer sensors have good performance at high humidity levels but are thermally unstable and have poor durability. Humidity sensors should be made up of material that shows high sensitivity, reproducibility, fast response and recovery time and cost-effectiveness. As MOFs pore extents are extremely distinct from other conventional substantial such as polymers, it can potentially engineer the highly ordered humidity sensors. For mentioned reasons, we decided in this work to investigate MOF-76(Gd) as a humidity sensor.

Humidity sensing recitation of the sample MOF-76(Gd) was appraised with several important sensing parameters. The variance method is used for %RH measurements. Fig. 1 (left) shows a linear increment for all the material, with varying %RH and out of these entire samples MOF-76(Gd) was observed for highly linear increment with maximum order change in resistance between 11-98% RH which portrays outstanding sensing properties of MOF-76(Gd). Fig. 1 (right) gives the response and recovery time. It can be seen, response time was attained within 11s, and the recovery time was observed within 2s. This clearly confirmed that the MOF-76(Gd) material is characterized by

enhanced response and recovery times which provides its utility in futuristic humidity sensing application. Fig. 2 (right) shows the hysteresis curve of sample-based %RH sensor in which one line with a downwards arrow represents the adsorption process from closed chambers of 11 %RH to 98 %RH and another line with the upwards arrow represent the desorption process take place from closed chambers of 98 %RH to 11 %RH. It is observed that adsorption and desorption lines are closely overlapped with each other showing negligible hysteresis. The hysteresis error (γH) was calculated by using the expression, $\gamma H = \pm \frac{\Delta H_{max}}{2F_{FS}}$, where, ΔH_{max} is the difference in output of the process of adsorption and desorption and F_{FS} is the full-scale output.

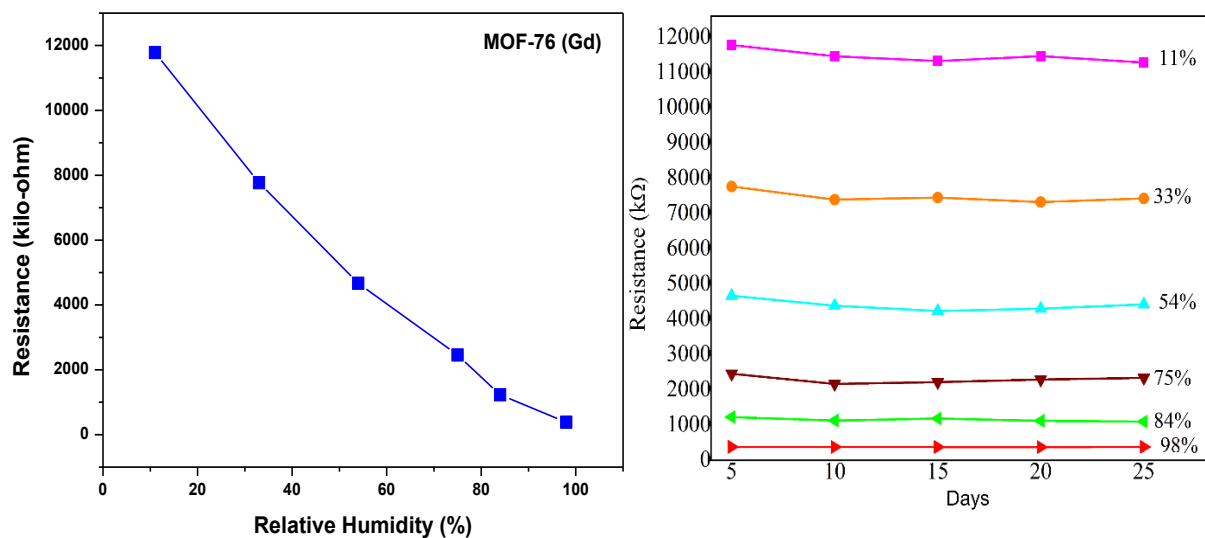


Figure 1: (left) Relative sensitivity of MOF-76(Gd) measured at each %RH. (right) Response of MOF-76(Gd) monitored at different humidity conditions for 30 days.

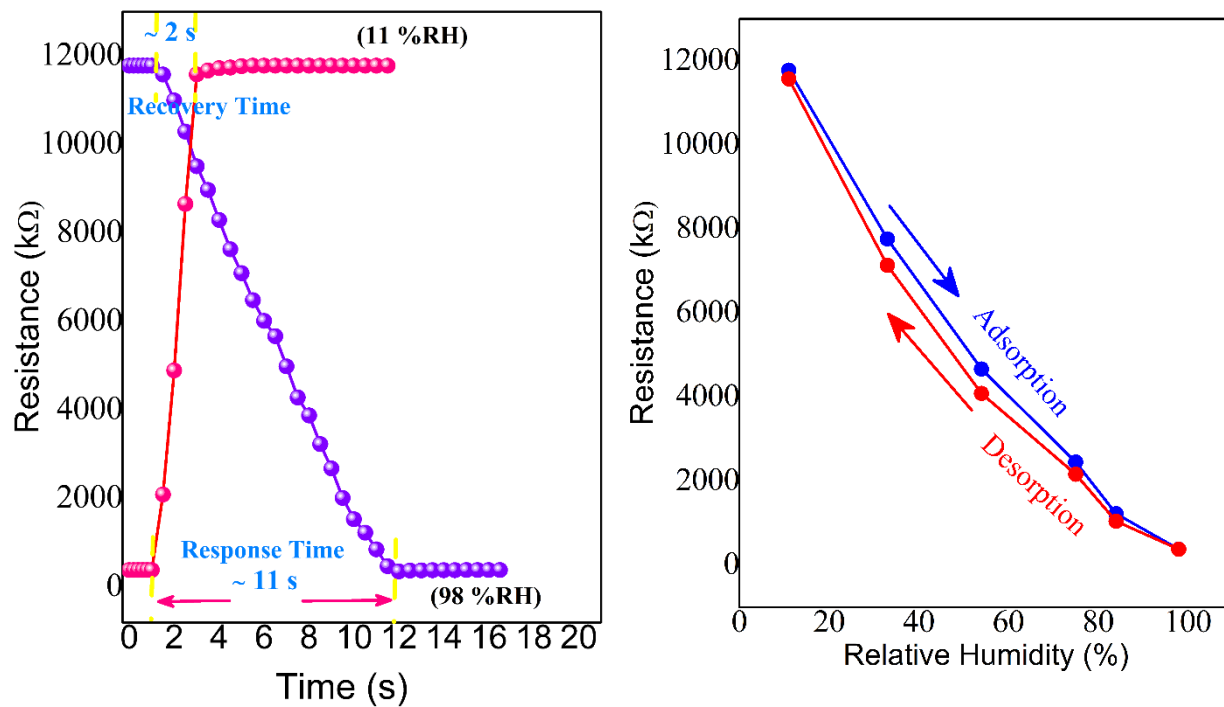


Figure 2: (left) Response/recovery time of the sensor MOF-76(Gd) measured between 11 %RH and 98 %RH. (right) Hysteresis curve showing adsorption-desorption responses measured in the 11-98 %RH range for MOF-76(Gd).

Acknowledgements

This work was supported by the projects: SK-CZ-RD-21-0068, VEGA-1/0294/22, KEGA-006UPJS-4/2021, VVGS-2022-2123 and TRIANGEL.

Hydrogen Storage and Humidity Sensing Using MOF-76(Tb)

A. Garg^a, R. Saini^b, A. Sharma^c, M. Almäši^{d*}

^a Department of Physics, Suresh Gyan Vihar University, Jaipur 302017 India

^b Department of Physics and Astrophysics, School of Basic Sciences, Central University of Haryana, Mahendergarh 123031 India

^c Department of Physics, School of Engineering & Technology, Central University of Haryana, Mahendergarh 123031 India

^d Department of Inorganic Chemistry, Faculty of Science, P. J. Safarik University, Moyzesova 11, Kosice 041 54 Slovak Republic

*miroslav.almasi@upjs.sk

Humidity sensors have many significant applications in daily life, such as medicine, biology, meteorology, agriculture and many others. Humidity sensors with accurate humidity control play a vital role in different industrial processes, food packaging, environmental monitoring, automotive control systems and equipment maintenance because of variations in moisture requirements. In recent years a lot of research works have been represented involving humidity sensors towards advance the performance. Humidity sensing materials comprising semiconductors, perovskite oxides, and polymers have attracted the attention of the scientific community presently. Among these materials, perovskite oxides humidity sensors based have shown high reliability and sensitivity. Many commercial humidity sensors are available to perceive volatile constituents at ppm-level concentrations but still, humidity sensing below ~100 ppm (few percentages relative humidity (RH) at 298 K) encounter challenges. In many applications such as medicinal provisions, gas and fuel storage, agricultural products storage, semiconductor manufacturing, humidity sensing is obligatory at ppm or ppb level.

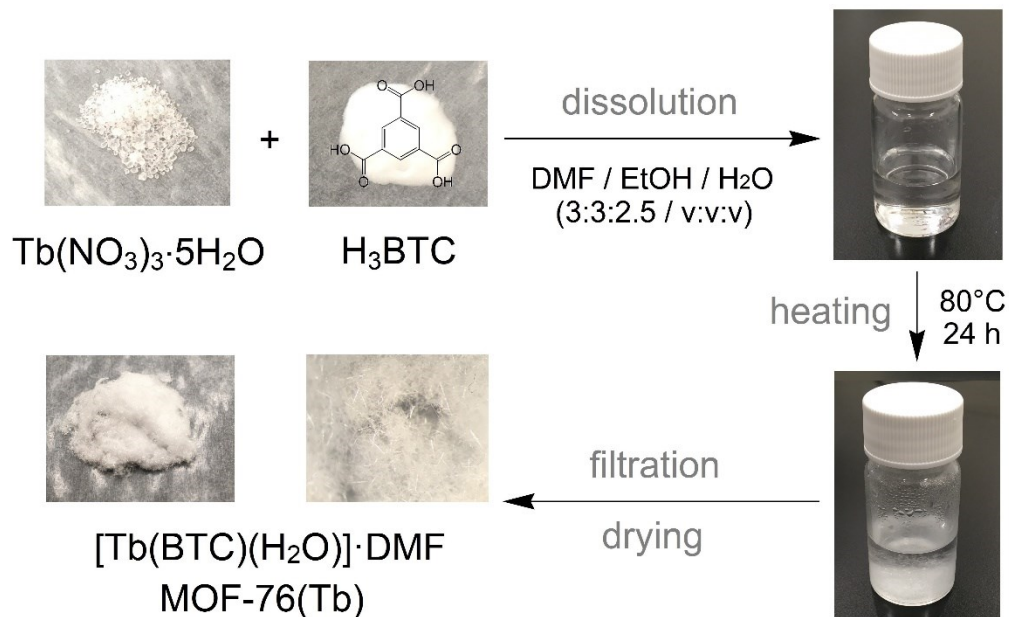


Figure 1: Individual steps of MOF-76(Tb) synthesis.

Synthesis (see Fig. 1) and characterization of MOF-76(Tb) and its application in hydrogen storage and humidity sensing application is represented in this research work. The maximal hydrogen storage capacity of MOF-76(Tb) was 0.6 wt. % at a pressure about 20 bar and 0.5 wt. % at 1 bar and 77 K. MOF-76(Tb) was mainly studied as a sensor for the detection of inorganic cations and anions, small organic molecules / pollutants and antibiotics. We tried to extend the sensing application of this compound to the adsorption of water molecules and its possible use as a humidity sensor. The activated compound MOF-76(Tb) contains coordinatively unsaturated sites (CUSs) located on Tb(III) ions, which are formed by the removal of coordinated water molecules after thermal activation of the material. Because CUSs serve as the primary sites for the adsorption process of different molecules, the prepared compound has also been studied as a humidity sensor. Humidity sensing measurements (see Fig. 2) indicate that compound MOF-76(Tb) displays very high impedance at low humidity conditions (11 % RH), however, a moderate decrement in impedance was shown at high humidity conditions (98 % RH). As can be seen from Fig. 1, the decreasing order in resistance of relative humidity could be ranged in the following order: 9868 k Ω at 11 % RH, 9017 k Ω at 33 % RH, 8642 k Ω at 53 % RH, 8003 k Ω at 75 % RH, 7431 k Ω at 84 % RH and 6137 k Ω at 98 % RH. The sample deviates from a linear response and for this reason, is not an ideal candidate for humidity sensing applications.

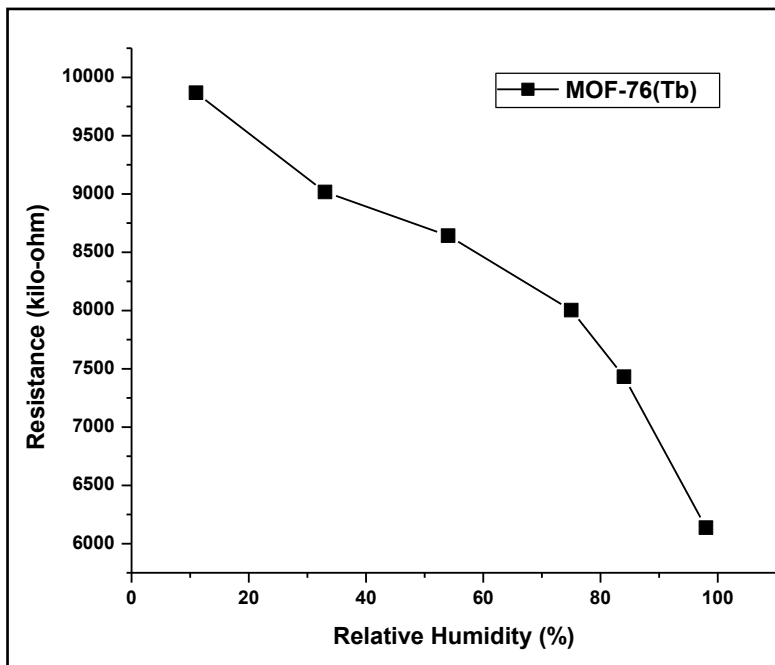


Figure 2: Humidity sensing curve of MOF-76(Tb).

Acknowledgements

This work was supported by the projects: SK-CZ-RD-21-0068, VEGA-1/0294/22, KEGA-006UPJS-4/2021, VVGS-2022-2123 and TRIANGEL.

Mesoporous Material MIL-101 as an Additive in LiS Batteries

D. Capková^a, T. Kazda^b, N. Király^c, A. Straková-Fedorková^a, M. Almási^{c*}

^a Department of Physical Chemistry, Faculty of Science, Pavol Jozef Safarik University, Moyzesova 11, 041 54, Kosice, Slovak Republic

^b Department of Electrical and Electronic Technology, Faculty of Electrical Engineering and Communication, Brno University of Technology, Technicka 10, 616 00, Brno, Czech Republic

^c Department of Inorganic Chemistry, Faculty of Science, Pavol Jozef Safarik University, Moyzesova 11, 041 54, Kosice, Slovak Republic

*miroslav.almasi@upjs.sk

Metal-organic framework MIL-101(Fe)-NH₂ was used in the present study as a matrix for sulphur cathode. The crystal structure of MIL-101(Fe)-NH₂ is built from 2-aminoterephthalate molecules as linkers and Fe(III) ions as nodes. Fe(III) ions are arranged in a trigonal planar cluster with composition [Fe₃(μ₃-O)(μ₂-COO)₆(H₂O)₂Cl] (COO = carboxylate) and a trigonal prismatic secondary building unit (SBU, see Fig. 1a). Four [Fe₃(μ₃-O)(μ₂-COO)₆(H₂O)₂Cl] clusters are bridged with six BDC-NH₂ anions under the formation of the structural unit, so-called supertetrahedron. The four vertexes of the supertetrahedron are occupied by the trigonal clusters, while the organic linkers are located at the six edges of the supertetrahedron with the length of vertex ~11 Å (see Fig. 1b). The connection of the units ensures a three-dimensional network of “corner-sharing” supertetrahedrons with an augmented MTN zeotype architecture. The final crystal structure of MIL-101(Fe)-NH₂ contains different cages with different sizes: a microporous cage with a free diameter for entrance windows close to 8.6 Å and two different mesoporous cages with a diameter close to 29 Å and to 34 Å, respectively (see Fig. 1c). Mesoporous cages consist of pentagonal and hexagonal windows, and the free opening of the smallest one is ~12 Å and for bigger one is ~14.5 and 16 Å. The resulting cubic structure exhibits several unprecedented features: a mesoporous MTN zeotype architecture, extraordinary cell volume, a hierarchy of extra-large pore sizes, large cage volumes and enormous sorption capacity toward different gases and large surface area (up to 4500 m² g⁻¹ BET).

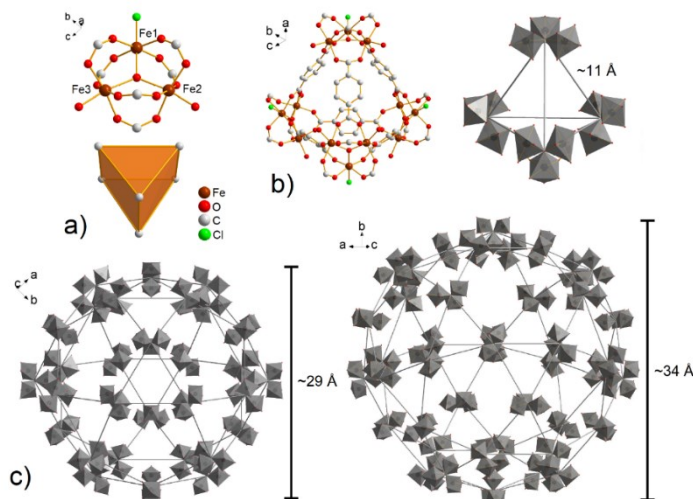


Figure 1: A view of the MIL-101(Fe)-NH₂ crystal structure: a) trigonal planar cluster of Fe(III) ions and corresponding trigonal prismatic secondary building unit, b) supertetrahedron formed from four cyclotrinuclear iron(III) clusters and six BDC-NH₂ linkers (hydrogen atoms and amine groups located on BDC-NH₂ molecules are omitted for clarity) and c) types of mesoporous cages located in the framework, smaller and larger cage with corresponding diameters.

Synthesis, characterisation, and electrochemical performance of cathodic material containing MIL-101(Fe)-NH₂ (C) as a host for sulphur were performed. It was demonstrated that MIL-101(Fe)-NH₂ (C) can be used as a conductive matrix for electrodes in lithium-sulphur batteries. The unique MOF structure can effectively absorb and mediate the redox reaction to better kinetic reaction and stable electrode structure. Active sulphur was captured and encapsulate into carbonized MIL-101(Fe)-NH₂ material for high-performance lithium-sulphur battery. The initial discharge capacity of the S/MIL/C/PVDF electrode was 775 mAh g⁻¹ at the current rate of 0.2 C and at fiftieth cycle 646 mAh g⁻¹ that corresponds to 83.3 % of original discharge capacity. The initial discharge capacity at the current rate 0.5 C was 705 mAh g⁻¹, after two hundred cycles it was 67.6 % of original discharge capacity, and the efficiency was around 95 % during this cycling (see Fig. 2). Results confirmed sustained cycle stability and low decay rate after 200 cycles. In addition, the specific support structure intercepted polysulphides was proven by the self-discharge testing. To study the electrochemical mechanism occurring between the electrode (S/MIL/C/PVDF) and electrolyte, electrochemical impedance spectroscopy (EIS) was performed. Different kinetic parameters of the electrode were calculated fitting EIS experimental data and obtained results were compared with other MOF materials. Finally, it can be concluded that MIL-101(Fe)-NH₂ (C) is a suitable host for sulphur and the described electrode is a promising material for applications in Li-S batteries.

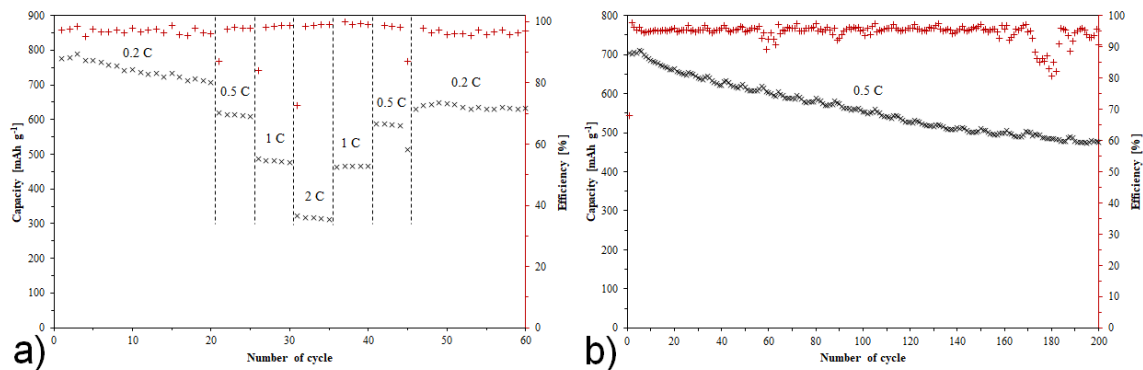


Figure 2: Capacity changes during cycling of S/MIL/C/PVDFelectrode: a) at different C-rates, b) 200 cycles at 0.5 C.

Acknowledgements

This work was supported by the projects: APVV-20-0138, SK-CZ-RD-21-0068, VEGA-1/0294/22, KEGA-006UPJS-4/2021, VVGS-2022-2123 and TRIANGEL.

Effect of MOF-76(Gd) Activation/Carbonization on the Cycle Performance Stability in Li-S Battery

D. Capková^a, T. Kazda^b, N. Király^c, A. Sharma^d, T. Zelenka^e, A. Straková-Fedorková^a, M. Almáši^{c*}

^a Department of Physical Chemistry, Faculty of Science, Pavol Jozef Safarik University, Moyzesova 11, 041 54, Kosice, Slovak Republic

^b Department of Electrical and Electronic Technology, Faculty of Electrical Engineering and Communication, Brno University of Technology, Technicka 10, 616 00, Brno, Czech Republic

^c Department of Inorganic Chemistry, Faculty of Science, Pavol Jozef Safarik University, Moyzesova 11, 041 54, Kosice, Slovak Republic

^d Department of Physics, School of Engineering & Technology, Central University of Haryana, 123031, Mahendergarh, India

^e Department of Chemistry, Faculty of Science, University of Ostrava, 30. dubna 22, 702 00 Ostrava, Czech Republic

*miroslav.almasi@upjs.sk

Herein, we report the synthesis, characterization and application of metal-organic framework material, gadolinium(III) benzene-1,3,5-tricarboxylate (MOF-76(Gd)) with an exact chemical formula $[\text{Gd}(\text{BTC})(\text{H}_2\text{O})]\cdot\text{DMF}$ (BTC = benzene-1,3,5-tricarboxylate, DMF = *N,N'*-dimethylformamide), as an conductive matrix in lithium-sulphur battery. The gadolinium(III) form of the MOF-76 family was chosen based on rapid preparation, high reaction yield and our positive experiences when we studied this material as a magnetic refrigerator, a humidity sensor and an adsorbent of carbon dioxide, methane and hydrogen. The choice of MOF-76(Gd) was also due to the electron configuration of Gd(III) ion, as it contains seven unpaired electrons in $4f$ orbital, which is the largest possible total spin ($S = 7/2$) within the elements in the periodic table. Due to this fact, Gd(III) compounds are intensively studied from a magnetic point of view, and we assumed a positive effect on the electrochemical properties. According to the best of our knowledge, the impact of Gd(III) ions in MOF materials on the electrochemical properties in Li-S batteries has not yet been studied and described. The electrode material dopped by Gd(III) ions in Li-ion batteries showed stable cycle performance with higher capacity compared to the absence of Gd(III) ions. According to the improved properties in Li-ion batteries and a gap in Li-S batteries, our choice for metal ion in a MOF-76 was gadolinium(III). MOF-76(Gd) was studied in an activated (AC) and carbonized (C) form, and the electrochemical behaviour of both materials as a sulphur matrix in the cathode of Li-S battery was investigated. In

order to prepare a more conductive matrix, MOF-76(Gd) was carbonized and applied into the cathode material in Li-S battery. The cathode with activated MOF-76(Gd) obtained an initial discharge capacity of 620.8 mAh g⁻¹ at 0.5 C and after 200 cycles, the capacity decreases down to 502.4 mAh g⁻¹ with the capacity fading rate of 0.096 % per cycle. The electrode with carbonized MOF-76(Gd) reached the value of 657.9 mAh g⁻¹ after 200 cycles maintaining the capacity of 610.2 mAh g⁻¹, and high cycling stability of only 0.036 % capacity decay per cycle was achieved (see Fig. 1).

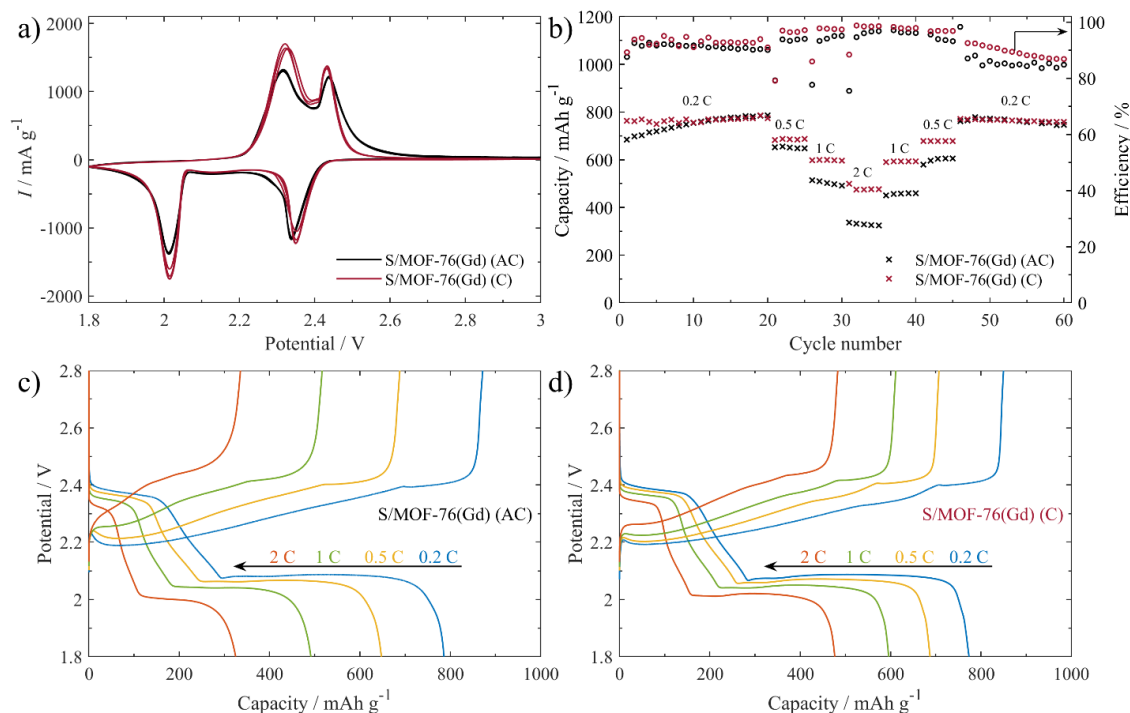


Figure 1: a) CV curves of the S/MOF-76(Gd) (AC) and S/MOF-76(Gd) (C) electrodes at scan rate of 0.1 mV s⁻¹, b) Galvanostatic cycling of the S/MOF-76(Gd) (AC) and S/MOF-76(Gd) (C) electrodes from 0.2 C to 2 C, Galvanostatic charge/discharge profiles of c) the S/MOF-76(Gd) (AC) and d) S/MOF-76(Gd) (C) electrodes cycled between 1.8 V and 2.8 V at various current densities.

Acknowledgements

This work was supported by the projects: APVV-20-0138, SK-CZ-RD-21-0068, VEGA-1/0294/22, KEGA-006UPJS-4/2021, VVGS-2022-2123 and TRIANGEL.

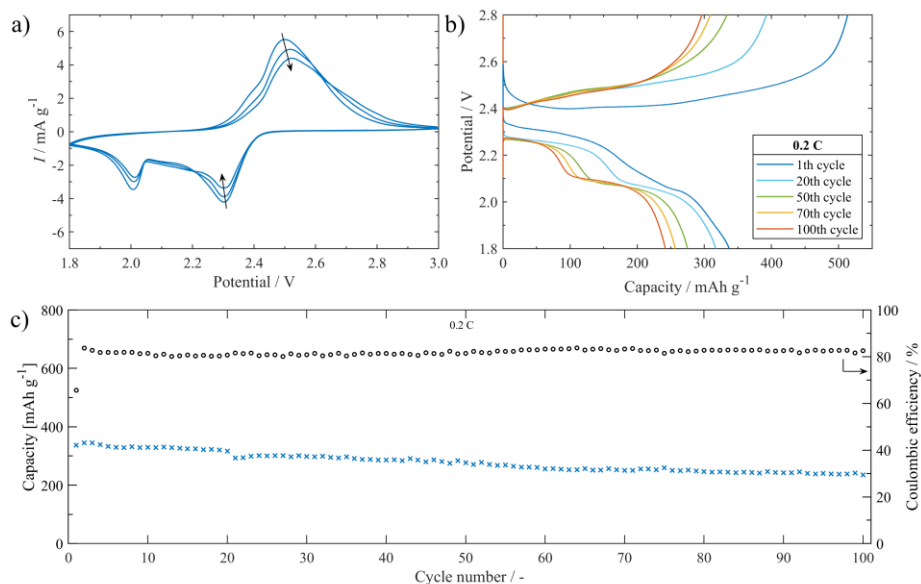
Sr(II) and Ba(II) Alkaline Earth Metal-Organic Frameworks (AE-MOFs) as Materials for Energy Storage and Selective Gas Adsorption

N. Király^a, D. Capková^b, T. Kazda^c, R. Gyepes^d, T. Zelenka^e, M. Almási^{a*}

- ^a Department of Inorganic Chemistry, Faculty of Science, Pavol Jozef Safarik University, Moyzesova 11, 041 54, Kosice, Slovak Republic
- ^b Department of Physical Chemistry, Faculty of Science, Pavol Jozef Safarik University, Moyzesova 11, 041 54, Kosice, Slovak Republic
- ^c Department of Electrical and Electronic Technology, Faculty of Electrical Engineering and Communication, Brno University of Technology, Technická 10, 616 00, Brno, Czech Republic
- ^d Department of Inorganic Chemistry, Faculty of Science, Charles University, Hlavova 2030, 128 00 Prague, Czech Republic
- ^e Department of Chemistry, Faculty of Science, University of Ostrava, 30. dubna 22, 702 00 Ostrava, Czech Republic

*miroslav.almasi@upjs.sk

In the present study, two novel alkaline earth metal-organic frameworks (AE-MOFs) consisting of Sr(II) (**UPJS-15**) / Ba(II) (**UPJS-16**) ions and extended tetrahedral tetraazotetracarboxylic acid (H₄MTA) were prepared and characterized in detail. Single-crystal X-ray analysis showed that the compounds are isostructural and their crystal structures are formed by alkaline-earths ions, which are arranged in 1D chains bridged by MTA linkers. In the frameworks, one-dimensional channels with sizes of 11.19 × 10.10 Å² for **UPJS-15 (AS)** and 10.69 × 9.70 Å² for **UPJS-16 (AS)** are present, which are filled with solvent molecules (DMF, H₂O). Solvents in the channels were exchanged for a lower boiling solvent, ethanol for easier and efficient activation. Prepared MOFs were characterized by the combination of EA, ICP-MS, IR, DRIFT, TG, PXRD, HE-PXRD, TEM and EDS. The process of compounds activation was studied by a combination of *in-situ* heating DRIFT, TG and *in-situ* heating HE-PXRD, which confirmed the stability of compounds after desolvation. The materials were subsequently studied as adsorbents of various gases (N₂, Ar, CO₂ and H₂) and the results obtained were compared with other MOFs containing tetrahedral ligands. Argon and nitrogen adsorption measurements revealed that **UPJS-15** exhibits *S*_{BET} surface area of 1250 m² g⁻¹ (N₂) / 1321 m² g⁻¹ (Ar) and **UPJS-16** adsorbs only limited amounts of adsorbates. However, both materials adsorb CO₂ with maximum capacities of 22.4 wt.% (5.08 mmol g⁻¹) at 0 °C; 14.7 wt.% (3.34 mmol g⁻¹) at 20 °C and 101 kPa for **UPJS-15** and 11.5 wt. % (2.63 mmol g⁻¹) at 0°C; 8.4 wt. % (1.89 mmol g⁻¹) at 20 °C and 101 kPa for **UPJS-16**. The adsorption active sites within the central atoms and the linker molecule were studied by DFT modelling. The calculations confirmed that the primary sites of adsorption are coordination unsaturated sites (CUSs) located on the central atoms ($\Delta H = -60.81$ kJ mol⁻¹) and azo groups ($\Delta H = -19.05$ kJ mol⁻¹) / phenyl rings ($\Delta H = -19.32$ kJ mol⁻¹ for CO₂ ⋯ π interaction and $-\Delta H = -7.80$ kJ mol⁻¹ for CO₂ ⋯ H-C interaction) within the MTA linker. According to IAST calculation, **UPJS-16** displays



considerable selectivity at low pressure with a maximum at 455 for CO_2/N_2 equimolar binary mixture and 50 for CO_2/N_2 10:90 mixture. Calculated results showed that the compound can adsorb large amounts of CO_2 from the air even at low pressures. This observation is especially important in the selective capture of CO_2 and the reduction of its concentration in the atmosphere, which is crucial from the point of view of environmental applications to reduce global warming. From an energy storage perspective, the materials have been studied as hydrogen adsorbents, but the compounds show small adsorbed amounts of H_2 , 0.19 wt.% (0.94 mmol g^{-1}) for **UPJS-15** and 0.04 wt.% (0.19 mmol g^{-1}) for **UPJS-16** at $-196 \text{ }^\circ\text{C}$ and 1 bar. On the other hand, the increased CO_2/H_2 selectivity could be used to purify hydrogen from carbon dioxide in WGS and DSR reactions. The second way of presenting materials in the energy storage area was the application of **UPJS-15** as an additive in a lithium-sulfur battery. The cycling performance at a cycling rate of 0.2 C shows the initial discharge capacity of 337 mAh g^{-1} and decrease continuously to 235 mAh g^{-1} after 100 charge/discharge cycles with a capacity retention of $\sim 70 \%$ (see Fig. 1). Nevertheless, the material shows slightly lower capacity compared to other MOF materials in the sulfur cathode, the capacity retention at the end of cycling was higher.

Figure 1: a) The cycling voltammogram of the **S/UPJS-15** cathode at 0.1 mV s^{-1} between 1.8-3.0 V. b) Charge and discharge curve platform during cycling at 0.2 C between 1.8-2.8 V. c) Cycling performance of the cell with the **S/UPJS-15** cathode at 0.2 C for 100 cycles.

Acknowledgements

This work was supported by the projects: APVV-20-0138, SK-CZ-RD-21-0068, VEGA-1/0294/22, KEGA-006UPJS-4/2021, VVGS-2022-2123 and TRIANGEL.

Electrochemical oxidation of industrial pollutants in groundwater from landfill of chemical waste disposal site CHZJD Bratislava-Vrakuňa

Gergő Bodnár^{a*}, Daniel Kupka^a

^a Institute of geotechnics, Slovak Academy of Sciences, Watsonova 45, Košice 04001

*bodnar@saske.sk

25

This work deals with the electrochemical oxidation of industrial pollutants in groundwater samples from landfill of chemical waste disposal site CHZJD Bratislava-Vrakuňa.

The toxic waste landfill of former Juraj Dimitrov chemical plant (CHZJD) is located in the districts of Bratislava - Ružinov and Vrakuňa. Approximately 90 000 m³ of chemical waste is buried under the surface. Because of the lack of constructing an isolating barrier dangerous substances are transported downstream by the groundwater flow. The location of the landfill threatens the biggest fresh groundwater reservoir in central Europe [1].

The electrolysis of groundwater samples from the geological borehole HGSV-10 was performed under galvanostatic conditions in an undivided electrochemical cell. Niobium mesh coated with a boron doped diamond layer (BDD) were used as electrode material. The geometric area of the BDD electrodes were 65 mm x 225 mm. The electrolysis was carried out at room temperature in a batch mode at current density 100 A m² (180 min).

The solution was mixed by up-flow gas lifting. During electrochemical treatment, the liquid samples were withdrawn from the electrolytic cell at regular intervals for TOC, COD, ion-chromatographic and mass spectrometric analyses.

During the electrolysis of groundwater, the COD decreased within 180 minutes from an initial concentration of 396 mg L^{-1} to a concentration below the analytical method detection limit ($5,10^{-1} \text{ mg L}^{-1}$) and the TOC concentration decreased to 20% of its initial value, from $169,6 \text{ mg L}^{-1}$ to $39,80 \text{ mg L}^{-1}$.

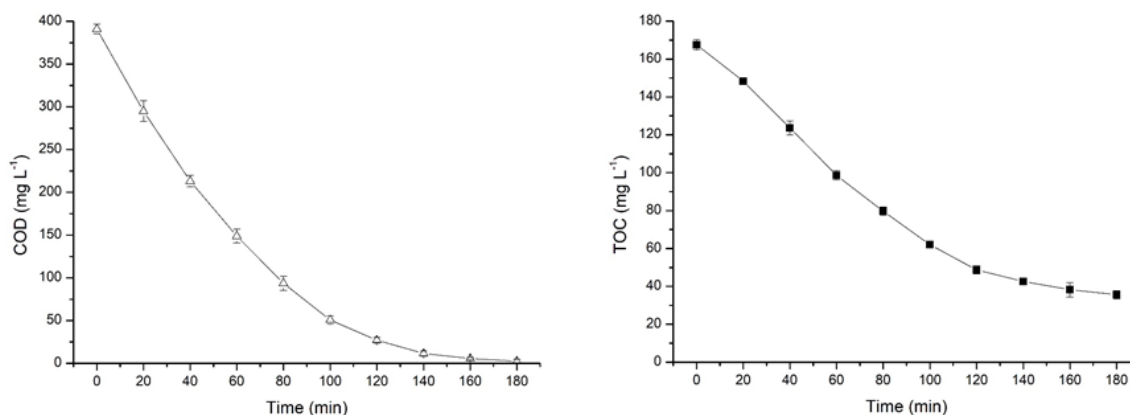


Figure 1: Decrease of COD and TOC during ELT of a groundwater sample from geological borehole HGSV-10.

Groundwater samples of target analytes were analyzed by HPLC Dionex Ultimate 3000 on reversed phase columns (Acclaim™ 120-C18, 3 μm, 120 Å, 2,1 x 100 mm, Thermo Scientific). Mixture of methanol (LC-MS grade) and ultrapure water was used as mobile phase. The separated molecules were detected with Diode array detector (DAD) and mass spectrometry with electron spray ionization (ESI-MS micrOTOF-Q II™ Bruker Daltonics) in positive mode and negative mode. The chemical composition of groundwater contamination caused by the CHZJD-Vrakuňa chemical landfill is heterogeneous and can be characterised by several main groups such as chlorinated hydrocarbons, phenolic substances, rubber chemicals based mainly on benzothiazole and pesticides. Overall 42 analytes were identified by HPLC-MS. The unequivocal confirmation of the target analytes was accepted only if the m/z value of the parent ion and the m/z value of least two fragmentation ions was in the 5 ppm error difference.

During the experiment, the efficiency of electrochemical oxidation of contaminants in groundwater under the chemical waste landfill CHZJD Vrakuňa - Bratislava was monitored. Several basic parameters such as pH, conductivity, TOC, COD and inorganic salt concentrations were monitored to confirm the efficiency of the electrochemical

process. The decrease in COD and TOC concentration and increase in nitrate and sulfate concentration confirmed the mineralization of organic contaminants. HPLC-MS technique was used to confirm the oxidation efficiency of organic contaminants. The contaminant removal efficiency was in the range of 70-90%. Advanced electrochemical oxidation processes (EAOP) such as electrochemical oxidation using BDD electrodes represents a modern and efficient treatment technology that is able to destruct persistent organic pollutants in aqueous media.

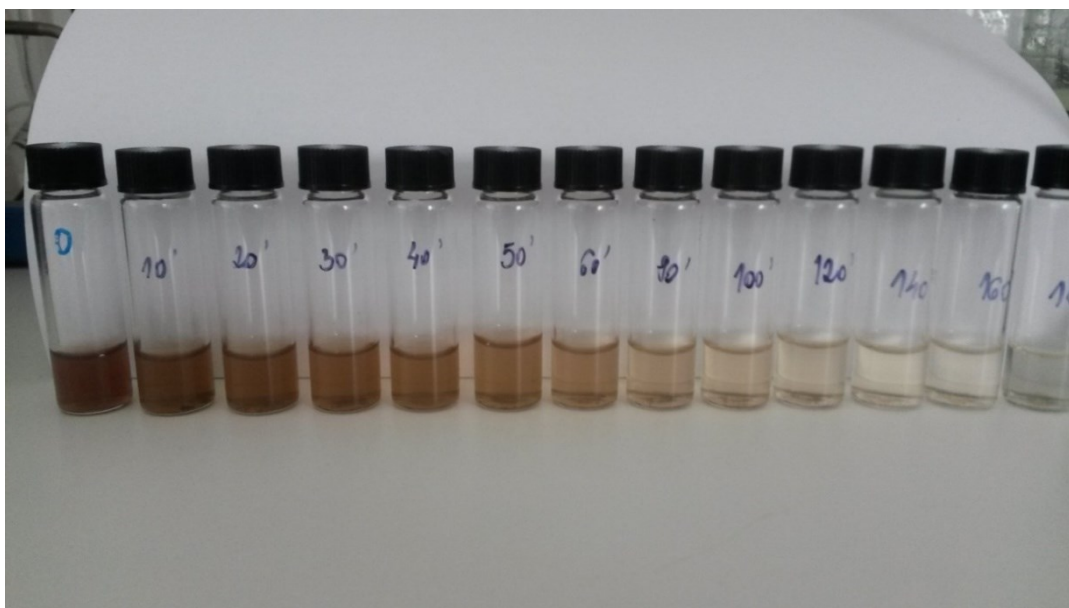


Figure 2: Color change of ground water during the electrolysis.

Acknowledgements

This work has been supported by: project APVV-19-0302 (COMWAT) Hybrid Composites for Complex Treatment of Industrial Waters

Project VEGA 2/0142/19: Study of the bio-oxidising and bio-reducing processes of sulphur and its compounds in environment and industry

Project BSK, SAV a PriF UK na výskum možností dekontaminácie environmentálnej záťaže Bratislava - Vrakuňa - Vrakunská cesta, skládka CHZJD“

References

[1] E-J, E.S.I., Chemické závody Juraja Dimitrova., in Encyklopédia Slovenska II E-J. 1978, Veda: Bratislava.

Study of stability of molybdenum-nickel electrocatalyst for hydrogen evolution reaction in alkaline solution

Renata Bodnarova^a, Miroslava Kozejova^a, Vitalii Latyshev^a, Serhii Vorobiov^a and
Vladimir Komanicky^{a*}

^a Department of Condensed Matters Physics, Faculty of Science, P. J. Safarik
University, Park Angelinum 9, 041 54, Kosice, Slovak Republic
*renata.bodnarova@student.upjs.sk

In this work, we studied the catalytic activity of magnetron sputtered molybdenum-nickel thin films for hydrogen evolution reaction (HER) in alkaline aqueous electrolyte. The MoNi thin films were characterized by scanning electron microscopy and X-ray diffraction (XRD). The catalytic activity for HER and the stability of the MoNi alloys prepared by sputtering at room temperature and 800 °C was tested by cycling and chronoamperometry in 1M NaOH. Our results show that the catalytic activity of all Mo-Ni alloys prepared at elevated temperatures is significantly higher than the activity of pure metals. This point out to synergy effect between Ni and Mo. On the other hand, Mo-Ni alloys sputtered at room temperatures did not show any increased activity over pure Ni metal. The Mo₆₃Ni₃₇ alloy prepared at 800 °C shows catalytic activity and good stability.

Introduction

One of the most pressing challenges of modern society is finding a sustainable solution to the looming energy crisis. [1] In this quest electrochemistry plays an important role, since it provides new solutions for the conversion between electrical and chemical energy, thus enabling the storage of energy in the form of chemical bonds. [2] One of the most promising energy carriers is the hydrogen molecule. Water electrolysis is an environmentally friendly approach to hydrogen production. [3] Nickel alloys are characterized by high corrosion resistance and good catalytic properties. for hydrogen evolution reaction [4]. In this study, we focused on studying the stability of selected MoNi alloys with a precisely defined structure prepared by magnetron sputtering. Under the same conditions, it is a very reproducible method. Sputtered MoNi films exhibit good hardness, chemical, and mechanical resistance, and good electrical conductivity. [5]

Experimental

The MoNi alloys were cycled several times. For this study, we selected alloy with composition $\text{Mo}_{63}\text{Ni}_{37}$. We chose this particular composition since it shows one of the best activities for HER. The activity of the $\text{Mo}_{63}\text{Ni}_{37}$ thin layer for HER changed significantly during cycling (from 0.1V to -0.3 V vs. Ag/AgCl in 1M NaOH with a scan rate of $50\text{mV}\cdot\text{s}^{-1}$). The overpotential value of the MoNi sample was changed by 80 mV from 1st to 100th cycle (overpotential corrected for internal resistance). The data were corrected by IR correction to obtain a graph of the polarization curves in Figure 1a. Another suitable method for characterizing catalyst stability is chronoamperometry, (Figure 1b). The main principle of the method is to set a constant potential and monitor the dependence of the current on time. We choose the potential so that the current densities are greater than $10\text{mA}\cdot\text{cm}^{-2}$. Initially, we observed a higher activity and after 3500 seconds it decreased about 75 percent. In this part, a thin layer of MoNi dissolves into the electrolyte. By visual examination, it seems that a decrease of activity is caused by peeling off the thin films from the substrate. The improvement of the adhesion is needed which is a subject of further experiments.

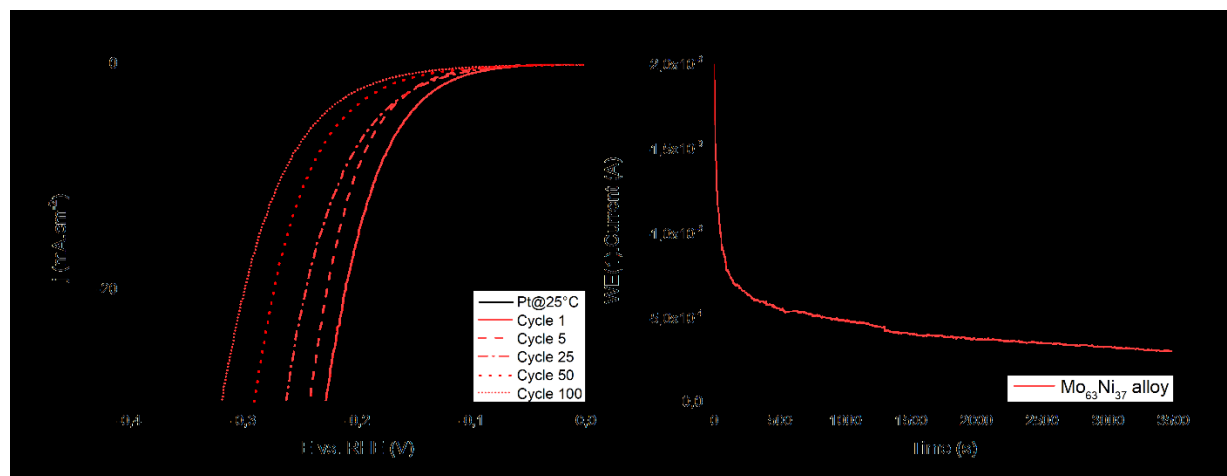


Figure 2: Catalyst stability test a) polarization curves obtained by cycling a) $\text{Mo}_{63}\text{Ni}_{37}$ and b) chronoamperometric curve of $\text{Mo}_{63}\text{Ni}_{37}$ sample.

Conclusion

The results in this report demonstrate the design of MoNi catalysts with high activity for hydrogen evolution in alkaline solution. The alloy with the best activity has the composition $\text{Mo}_{63}\text{Ni}_{37}$. Also, catalysts prepared with a significantly higher amount of Mo 60 % in the sample show better HER activity and stability as a catalyst with more than 60 % of Ni. According to our stability measurements, the decrease of catalyst activity was not due to an intrinsic reduction of its activity but rather a result of the catalyst peeling off the substrate.

Acknowledgements

This work has been supported by grant 313011V334, Innovative Solutions for Propulsion, Power and Safety Components of Transport Vehicles, and grants of the Slovak Research and Development Agency under contract APVV-20-0324.

References

[1] N. Armaroli, et al. The future of energy supply: challenges and opportunities." In *Angewandte Chemie International Edition*, **46** (2007), 52-66.

[2] Z. Yang, et al. Electrochemical energy storage for green grid. " In *Chemical Reviews*, **15** (2011), 3577-3613.

[3] X. Zou, et al. Noble metal-free hydrogen evolution catalysts for water splitting." In *Chemical Society Reviews*, **15** (2015), 5148-5180.

[4] Y. Wang, et al. "Structural stability of Ni-Mo compounds from first-principles calculations. " In *Scripta Materialia*, **1** (2005),17-20.

[5] N. S. Lewis, et al. "Powering the planet: Chemical challenges in solar energy utilization." In *Proceedings of the National Academy of Sciences*, **43** (2006), 15729-15735.

Infiltration of Sulphur into a Porous Conductive Host Based on a Metal-Organic Framework and its Application as a Cathode in Li-S Batteries

D. Capkova^{a*}, T. Kazda^b, M. Almasi^c, O. Cech^b, N. Kiraly^c, K. Jasso^b, J. Macko^a, and A. Strakova Fedorkova^a

- ^a Department of Physical Chemistry, Pavol Jozef Safarik University in Kosice, 040 01
Kosice, Slovak Republic,
- ^b Department of Electrical and Electronic Technology, Brno University of Technology,
602 00 Brno, Czech Republic
- ^c Department of Inorganic Chemistry, Pavol Jozef Safarik University in Kosice, 040 01
Kosice, Slovak Republic

*dominika.capkova@upjs.sk

The energy density of lithium-ion batteries has proven insufficient in a future applications such as portable electronic devices, electric vehicles or satellites. Lithium-sulphur (Li-S) batteries with a theoretical capacity of 1675 mAh g⁻¹ are among the promising candidates to replace lithium-ion batteries [1].

Metal-organic framework material, gadolinium(III) benzene-1,3,5-tricarboxylate (MOF-76(Gd)) with an exact chemical formula [Gd(BTC)(H₂O)]·DMF (BTC = benzene-1,3,5-tricarboxylate, DMF = *N,N'*-dimethylformamide) was synthesized and applied as an additive as a host for sulphur in cathode material for Li-S battery. Sulphur was dissolved in carbon disulphide and infiltrated into the pores of MWCNTs. The final mass ratio of sulphur, MOF-76(Gd), carbon Super P, MWCNTs and polyvinylidene fluoride (PVDF) in the electrode material (electrode denoted as S/C/MOF-76(Gd)) was 60:12:12:6:10.

Electrochemical properties of prepared S/C/MOF-76(Gd) electrode were investigated by cyclic voltammetry and galvanostatic cycling. The results of the CV analysis are shown in Fig. 1a. Anodic and cathodic peaks are sharp and stable, with cycle numbers indicating fast redox kinetics. Anodic peaks can be observed around 2.32 V and 2.43 V and two cathodic peaks, related to the conversion of sulphur to higher and lower polysulphides, around 2.33 V and 2.0 V, respectively.

Subsequently, the cycle performance of the S/C/MOF-76(Gd) electrode was carried out at different current rates from 0.2 C to 2 C (see Fig. 1b). The S/C/MOF-76(Gd) electrode exhibits initial discharge capacity of 735 mAh g⁻¹ (4.22 mAh) at 0.2 C. After 20 cycles at 0.2 C the capacity increases up to 784 mAh g⁻¹ and the capacity retention was 106.6 %. The discharge capacities at 0.5, 1 and 2 C were 676, 581 and 432 mAh g⁻¹, respectively. When the current density shifts stepwise back from 2 C to 0.2 C, the discharge capacity at fiftieth cycle at 0.2 C was 788 mAh g⁻¹. The Coulombic efficiency despite the multi current density testing was around 96.8 %. The discharge capacity of the S/C/MOF-76(Gd) electrode is highly stable, with a capacity retention of 107.2 % in the fiftieth cycle.

Charge and discharge profiles at different current rates are illustrated in Fig. 1c. The shown charge/discharge curves are the last cycles of each current density. High and low voltage plateaus are clearly visible at all C-rates. With the increase of current density, the suppression of plateaus is improved. The characteristic potential barrier around 2.2 V during charging is visible at all current densities and strongly depends on the current rate. During discharging, the stable potential of high and low voltage plateau reached the lower value with increasing current density. A comparison of charge and discharge curves at 0.2 C during multi-current cycling is depicted in Fig. 1d. One can see that the discharge capacity is very stable, and the degradation of material during 50 cycles is negligible.

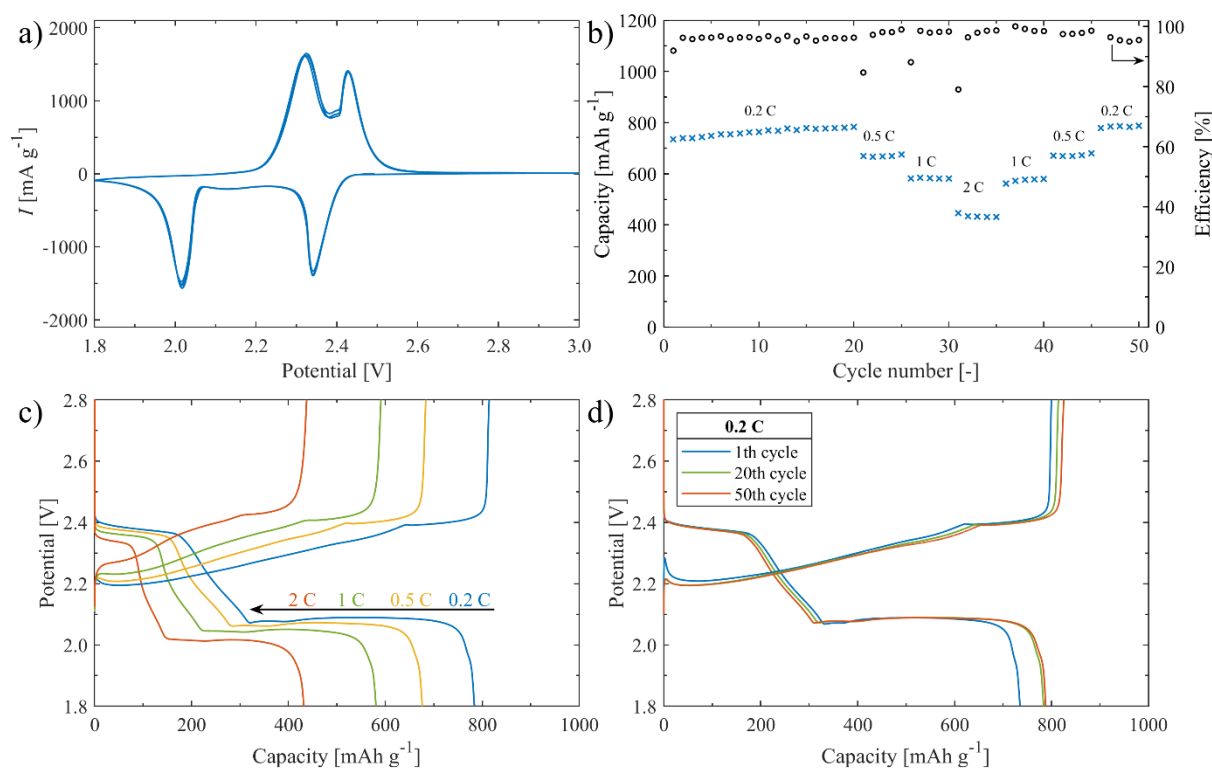


Figure 1: a) Cyclic voltammety of the S/C/MOF-76(Gd) electrode at scan rate of 0.1 mV s⁻¹, b) galvanostatic cycling of the S/C/MOF-76(Gd) electrode from 0.2 C to 2 C, galvanostatic charge and discharge profiles from c) multi-current cycling and d) cycling at 0.2 C.

Acknowledgements

This research was sponsored by the following projects: APVV-20-0138, Development of Novel 3D Materials for Post Lithium Ion Batteries with High Energy Density; APVV-20-0111, Towards Lithium Based Batteries with Improved Lifetime; iCoTS No. 313011V334, Innovative Solutions for Propulsion, Power and Safety Components of Transport Vehicles; vvg-pf-2021-1756, Development of Electrode Materials for Lithium-Sulfur

Batteries; VEGA 1/0074/17, Porous Coordination Polymers for Environmental Applications, and specific graduate research of the Brno University of Technology No. FEKT-S-20-6206.

References

[1] D. Capková, M. Almáši, T. Kazda, O. Čech, N. Király, P. Čudek, A. S. Fedorková, V. Hornebecq, *Electrochimica Acta* **354** (2020) 136640.

Voltammetric determination of ciprofloxacin in the flow system using a boron-doped diamond electrode

Olívia Dakošová^{a*}, Eva Melníková^a, and Miroslav Gál^a

^a Slovak University of Technology in Bratislava, Faculty of Chemical and Food Technology, Department of Inorganic Technologies and Materials, Radlinského 9, 812 37 Bratislava, Slovak Republic

*olivia.dakosova@stuba.sk

Abstract

In this study the voltametric behavior of ciprofloxacin (CIP) has been investigated at boron-doped diamond (BDD) electrode using cyclic voltammetry (CV) and square wave voltammetry. The measurements were performed in a flow cell, which was designed to stimulate the real flow system as accurately as possible. Various matrices were used to compare the redox behavior of CIP, such as 0.05 M PBS, river water sample and effluent wastewater sample. From the obtained data it is obvious that the flow rate has a significant impact on the electrochemical behavior of CIP. Compared to the stationary solution, we observed shifts in the value of peak potential and peak current as well.

Key words: Voltammetry, BDD electrode, Flow cell, Ciprofloxacin

Introduction

Wastewater is treated in wastewater treatment plants (WWTPs), which play an important role in improving the quality of the water before its return to the ecosystem [1]. In general, various contaminants enter the wastewater, but the emphasis in this work is on antibiotics, Due to the fact, that antimicrobial substances do not undergo complete degradation in the host organism, their original forms, metabolites, and transformation products are most often excreted in feces and urine and subsequently reach the WWTP. One of the most frequent antibiotics detected in the WWTP is ciprofloxacin (CIP). [2, 3]

Experimental

CIP of various concentration, 0.05 M PBS (both supplied by Merck), a river water sample taken from Červené Pleso, Slovakia and an effluent wastewater sample from WWTP Trnava, Slovakia were used. Cyclic voltammetry and square wave voltammetry were used to describe the electrochemical behavior of CIP at the BDD electrode in the above-mentioned matrices. To imitate the real flow system and to obtain more accurate results an electrochemical a flow cell was designed, in which the measurement itself took place. Measurements were performed using a Potentiostat PGSTAT 302N (Metrohm, Switzerland) and a software Autolab NOVA 2.1 (Metrohm, Switzerland) for the evaluation of the obtained data.

Results and discussion

Voltammograms (CV, SWV) recorded in all studied matrices are characterized by two irreversible oxidation peaks, where the first peak represents the oxidation of the amine group of ciprofloxacin (piperazine moiety) and the second one possibly refers to the attack of hydroxyl radicals on the quinolone moiety. Unlike the effluent wastewater sample, which as expected serves as a good electrolyte for the detection of CIP, in the case of the river water sample, probably due to its low conductivity, we observed very low and barely detectable oxidation peaks. A significant finding was that the position of individual oxidation peaks depends on the matrix in which the redox behavior of CIP was investigated. By analyzing cyclic voltammograms, we confirmed, that the reactions are diffusion controlled. Another important finding was the fact that the higher the concentration of CIP is in effluent wastewater, the more positive is the shift of oxidation peaks on the potential axes. The main purpose of this work was to study the effect of the flow rate and to compare these results with those of we obtained from stationary solution. With an increasing flow rate, there was a rise in both oxidation peak currents. This information is also very significant, because in the future it is planned to deploy such a monitoring device directly behind the WWTP, that can continuously monitor the content of environmentally hazardous substances.

Conclusion

This work focuses on the electrochemical behavior of CIP at the BDD electrode in the flow system. Compared to a stationary solution, we detected shifts in both peak height and peak potential. This means that by not considering the flow rate, we could get false results. To get accurate results it is necessary to carry out other measurements for various kinds of flow systems and subsequently compare the results.

Acknowledgements

This work was supported by the Slovak Research and Development Agency under the contract no. APVV-17-0149.

References

- [1] Morera, S., et al., Water footprint assessment in wastewater treatment plants. *Journal of Cleaner Production*, 2016. **112**, 4741-4748.
- [2] Birosova, L., et al., Pilot study of seasonal occurrence and distribution of antibiotics and drug resistant bacteria in wastewater treatment plants in Slovakia. *Sci Total Environ*, 2014. **490**, 440-4.
- [3] Chen, C., et al., Occurrence of antibiotics and antibiotic resistances in soils from wastewater irrigation areas in Beijing and Tianjin, China. *Environmental Pollution*, 2014. **193**, 94-101.

Electrochemical Deposition of Hydroxyapatite Coatings on the Zinc-based Substrates

R. Gorejová^{a*}, R. Oriňaková^a

^aDepartment of Physical Chemistry, Institute of Chemistry, Faculty of Science, P.J. Šafárik University in Košice, Moyzesova 11, 041 54, Košice

*radka.gorejova@student.upjs.sk

Metal-based absorbable materials represent a group of new progressive materials with potential use in recovery medicine. These will serve as temporarily degradable implants without the need to remove them from the body after the damaged tissue regeneration. One of the basic criteria for the success of such an implant is its biocompatibility and adequate host response. These properties can be improved by modifying the surface with suitable coatings. One of them is the hydroxyapatite (HAp) ceramic coating, which has been proven to improve the biocompatibility of the prepared materials [1,2]. At the same time, thanks to its human bone-like properties, it is a suitable candidate for such an application.

In this work, zinc-based materials with compositions of 100 wt.% zinc, 99 wt.% zinc-1 wt.% iron and 98 wt.% zinc-2 wt.% iron (Zn, Zn-1Fe, and Zn-2Fe, respectively) were prepared by cold-pressing from raw powders and subsequent sintering in an inert argon atmosphere. After that, these materials were grounded, ultrasonically cleaned in ethanol and acetone, and a hydroxyapatite layer was electrochemically deposited.

In the case of pure zinc, spindle-like crystals of HAp were deposited (Fig. 1a). On the other hand, more round-shaped and irregular Hap deposits were present on the samples made from Zn-Fe alloys (Fig. 1b,c). Different morphology and shape of the deposited HAp layer in presence of iron may be attributed to the different deposition potentials which arise from the different material bulk compositions. Different deposition conditions (current density, time of deposition e.g) along with the degradation and biological tests still need to be performed.

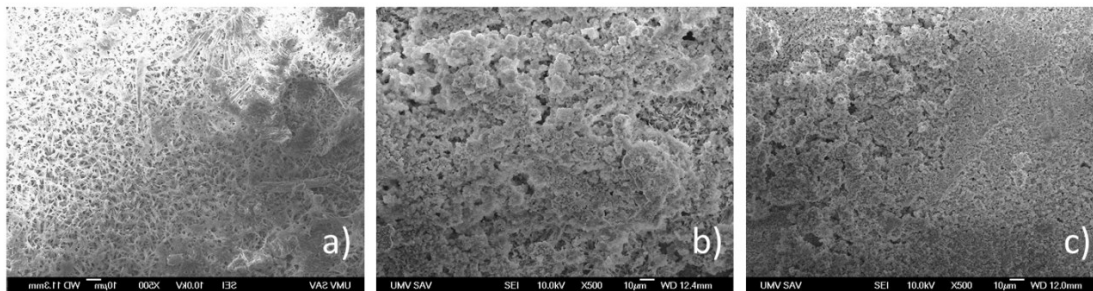


Figure 1: Hydroxyapatite coated Zn (a), Zn-1Fe (b) and Zn-2Fe (c) samples.

Acknowledgements

This work was supported by the Slovak Research and Development Agency (projects APVV-16-0029 and APVV-20-0278).

References

- [1] R. Oriňaková et al. *Int. J. Electrochem. Sci.* **10** (2015) 8158-8174.
- [2] W. S. W. Harun et al. *Ceramics International* **44** (2) (2018) 1250-1268.

Effect of thickness of NiCoP doped carbon fiber layers on their catalytic activity towards hydrogen evolution reaction

A. Gubóová^{a*}, R. Oriňaková^a, M. Strečková^b, C. Bera^b, O. Petruš^b, M. Paračková^a

^a Institute of Chemistry, Faculty of Science, P.J. Safarik University in Košice, Moyzesova 11, 040 01 Košice, Slovak Republic

^b Institute of Materials Research, Slovak Academy of Sciences, Watsonova 47, 040 01 Košice, Slovak Republic

*alexandra.guboova@student.upjs.sk

Advancement of renewable, suitable energy sources is highly researched nowadays due to always increasing demand for energy, rather rapid depletion of fossil fuels as well as the contamination of environment caused by these fossil fuels. Hydrogen is one of the most important ones among renewable energy sources because it has great energy value and is environmentally friendly [1]. The essential global challenge is now development of earth-abundant, superior performance capable and cost-effective catalyst for hydrogen evolution reaction [2].

Transition metal phosphides (TMPs) incorporated in carbon fibers (CF) are considered promising catalysts for hydrogen evolution reaction (HER) due to low cost, high activity and good stability. To understand their exceptional activity and perspective real use, behavior of these samples must be investigated in the form of thin porous layers that could be used directly in the proton-exchange membrane (PEM) electrolyser. Samples containing polyacrylonitrile (PAN) and mixture of polyacrylonitrile and polyvinyl pyrrolidone (PAN-PVP) were labeled NiCoP-CF-PAN and NiCoP-CF-PAN-PVP (Fig. 1). They were prepared by sintering electrospun carbon fibers doped with TMPs in the form of a thin layer with a thickness of few hundred micrometers (0.5mm and 0.2mm).

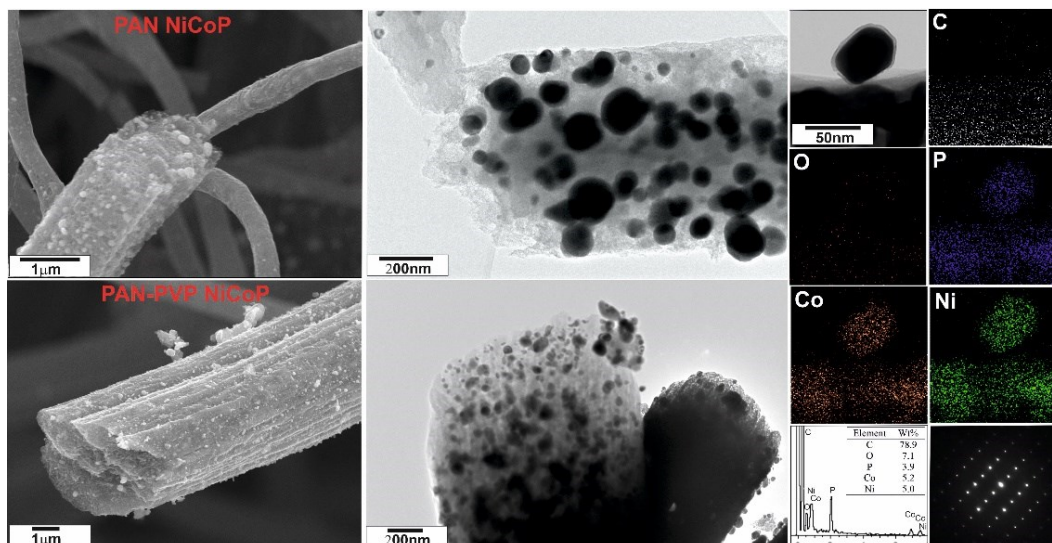


Figure 3: SEM images with clearly visible NiCoP nanoparticles and XRD analysis of NiCoP-CF-PAN and NiCoP-CF-PAN-PVP fibres.

The samples were initially characterized in a classical three- electrode setup in acidic (0.5M H₂SO₄) and alkaline (0.1M KOH) medium. The fibers in form of a layer were connected as a working electrode.

The fibers in the 0.5mm layer showed very good catalytic activity in acidic solution. In an alkaline environment, their activity was slightly worse, and the current densities were lower, which was even more pronounced in thinner (0.2mm) layers. As it can be seen from graphs in Fig. 2, when measured in a three-electrode setup, 0.2mm layers showed decrease in activity which may be due to a smaller active area or a smaller number of NiCoP catalytic nanoparticles.

However, it is important to note that behavior in a three-electrode system under laboratory conditions cannot be fully compared to the behavior of these layers in the cell. A thinner layer could be more advantageous in an electrolyser, as it allows easier removal of gas bubbles, which can greatly affect the overall performance. Therefore, the samples will be tested as a cathode catalyst for a PEM electrolyser.

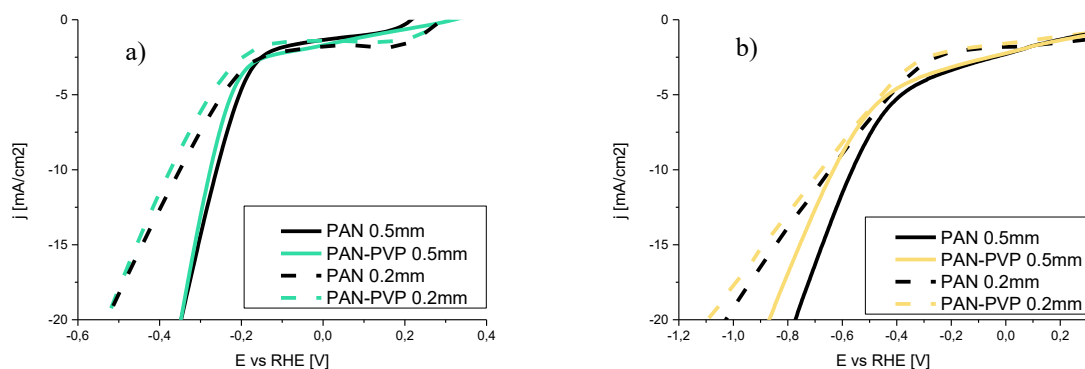


Figure 4: Polarization curves NiCoP CF in a) acidic media and b) alkaline media.

Acknowledgements

This work was supported by Grant Agency of Slovak Academy of Sciences, project no. VEGA 1/0095/21 (Application of innovative nano catalysts and DFT simulations for efficient hydrogen production), Slovak Research and Development Agency under the contracts no. APVV-20-0299 (Electrocatalysts for efficient hydrogen production for future electrolyzers and fuel cells) and no. APVV-20-0576 (Green ambitions for sustainable development (European Green Agreement in the context of international and national law)).

References

- [1] Hao Lv et al., Ultrathin PdPt bimetallic nanowires with enhanced electrocatalytic performance for hydrogen evolution reaction in *Applied Catalysis B: Environmental*, **238** (2018) 525-532.
- [2] B. Darband et al., Electrodeposited NiCoP hierarchical nanostructure as a cost-effective and durable electrocatalyst with superior activity for bifunctional water splitting in *Journal of Power Sources*, **429** (2019) 156-167.

Analytical characteristics of screen-printed carbon electrode modified by polypyrrole and NiO nanoparticles as a sensor for insulin determination

F. Chovancová^{*a}, I. Šišoláková^a, J. Shepa^a, R. Oriňaková^a

^a Department of Physical Chemistry, Faculty of Science, Pavol Jozef Šafárik University, Moyzesova 11, 04011 Košice, Slovak Republic

* frederika.chovancova1@student.upjs.sk

The biosynthesis of insulin appears by cleavage of single chain proinsulin containing 81 amino acids to insulin which consists of two chain connected by disulphide bridges. It is formed in the β -cells of the islets of Langerhans located in pancreas. [1-3]. Diabetes mellitus (DM) is considered as a global pandemic with rapidly increasing incidences nowadays. DM is a chronic metabolic disease represented by high glucose level in the blood. Incorrect control of patients with diabetes can result in serious lifelong complications [4]. Because of it, it is necessary to monitor the glucose or insulin level. Commercially the enzymatic glucose sensors are currently used for diabetes diagnosis [5]. However, these sensors faced some problems like stability or the high price of an enzyme non-enzymatic sensors are developed for diabetes diagnosis for insulin or glucose determination [6].

Nowadays, various analytical methods are used for insulin determination like as radioimmunoassay (RIA) [1], high-performance liquid chromatography (HPLC) [7] or enzyme-linked immunosorbent assay (ELISA) [8]. Regrettably, these methods are time consuming and require expensive instrumentations [8].

Therefore, research is focused on the development of non-enzymatic electrochemical insulin sensors. Electrochemical methods display great analytical characterizations like high sensitivity [8], fast analysis [9], low limit of detection [10] and inexpensive instrumentations [11].

This work deals with the determination of analytical characteristics of the screen-printed carbon electrode modified by polypyrrole and NiO nanoparticles (NiONPs/PPY/SPCE) to insulin determination. Analytical characteristics of NiONPs/PPY/SPCE were studied via cyclic voltammetry. The measurements were performed in 0.1 M NaOH and PBS with the scan rate of 0.1 V/s. Limit of detection (LOD) of prepared electrode was calculated as 0.047 μ M. The linear range of insulin concentration was determined 0.5 μ M to 5 μ M of insulin and value of correlation coefficient of $R^2 = 0.99$ was observed for

NiONPs/PPY/SPCE. Moreover, sensitivity was found at 0.0106 mA/ μ M. Therefore screen-printed carbon electrodes modified by nanoparticles NiONPs/PPY/SPCE are showed suitable analytical properties as a new sensor for insulin determination.

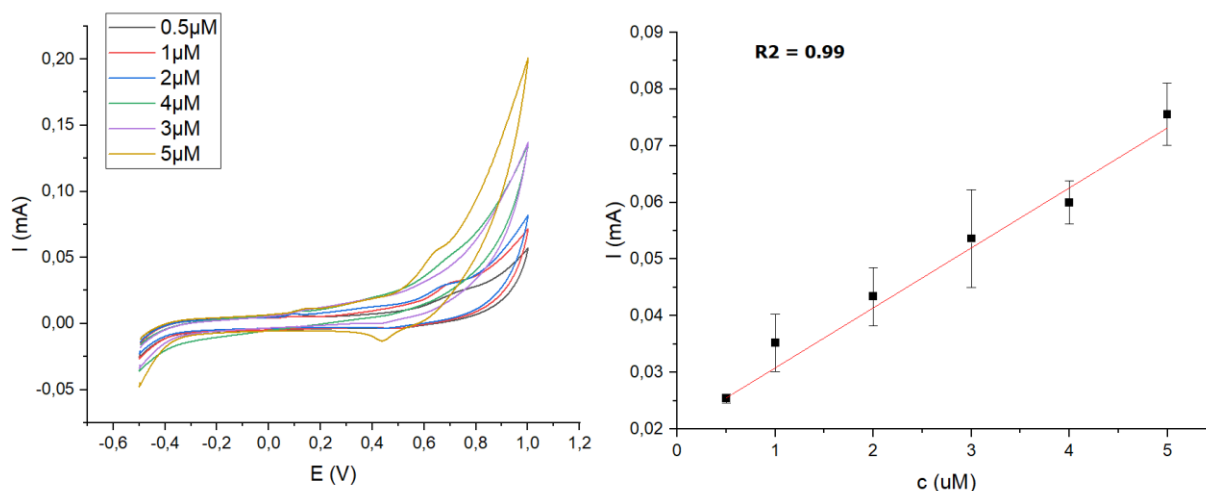


Figure 5: Cyclic voltammogram of 0.5 μ M - 5 μ M insulin of 0.1 M NaOH, PBS and scan rate 0.1 V/s at NiONPs/PPY/SPCE (left). The linear plot of insulin oxidation peak current vs concentration at NiONPs/PPY/SPCE (right).

Acknowledgements

This work has been supported by the APVV-PP-COVID-20-0036 and Visegradfound projectnumber 22020140.

References

- [1] A. Thomas, M. Thevis, Elsevier Inc. **93** (2019).
- [2] D. C. Simonson, Textb. of Nephro-Endocrinology (2009) 383–409.
- [3] S. Y. Tan, J. L. M. Wong, Y. J. Sim, S. S. Wong, S. A. M. Elhassan, S. H. Tan, G. P. L. Lim, N. W. R. Tay, N. C. Annan, S. K. Bhattamisra, M. Candasamy, Diabetes Metab. Syndr. Clin. Res. Rev. **13** (2019) 364–372.
- [4] G. Páth, N. Perakakis, C. S. Mantzoros, and J. Seufert, Metabolism. **90** (2019) 1–15.
- [5] J. Hovancová, I. Šišoláková, P. Vanýsek, R. Oriňaková, I. Shepa, M. Kaňuchová, N. Király, M. Vojtko, P. Čudek, A. Oriňák, *J. Electroanal. Chem.* **878** (2020).

- [6] J. Hovancová, I. Šišoláková, R. Oriňaková, A. Oriňák, (2017) 2147–2166.
- [7] I. Šišoláková, J. Hovancová, R. Oriňaková, A. Oriňák, L. Trnková, D. R. Garcia, J. Radoňák, *Bioelectrochemistry*. **130** (2019).
- [8] I. Šišoláková, J. Hovancová, R. Oriňaková, A. Oriňák, L. Trnková, I. Třísková, Z. Farka, M. Pastucha, J. Radoňák, *J. Electroanal. Chem.* **860** (2020).
- [9] I. Šišoláková, J. Hovancová, F. Chovancová, R. Oriňaková, A. Oriňák, J. Radoňák, *Electroanalysis*. (2020).
- [10] J. Yang, J. H. Yu, J. Rudi Strickler, W. J. Chang, S. Gunasekaran, *Biosens. Bioelectron.* **47** (2013) 530–538.
- [11] C. I. L. Justino, T. A. Rocha-Santos, A. C. Duarte, *TrAC - Trends Anal. Chem.* **29** (2010) 1172–1183.

PSM of Microporous Gallium-Porphyrin Frameworks for Gas Adsorption and Energy Storage in Li-S Batteries

N. Király^{a*}, D. Capková^b M. Almáši^a, A. Straková Fedorková^b, V. Zeleňák^a,

^a Department of Inorganic Chemistry, Faculty of Sciences, Pavol Jozef Šafárik University in Košice, Moyzesova 11, 04154, Košice, Slovak Republic

^b Department of Physical Chemistry, Faculty of Sciences, Pavol Jozef Šafárik University in Košice, Moyzesova 11, 04154, Košice, Slovak Republic

*nikolas.kiraly@student.upjs.sk

Introduction

In the field of crystalline porous materials, metal–organic frameworks (MOFs) exhibit tuneable pore sizes and surface chemistry, which in turn lead to a wide range of chemical and physical properties [1]. Hence MOFs are investigated in applications such as gas storage and separation, catalysis, and drug delivery [2]. In our quest for discovering novel original porous frameworks with multifunctional linkers, we mainly focused on porphyrinic building blocks. When porphyrins are used as building blocks for MOFs, facile molecular modification of porphyrins expands the possibilities of the structural design. Post-synthetic modification (PSM) of the metal-porphyrin frameworks by the introduce various metal sites into the pore surface of MOFs without alteration of the framework topology. In addition, the physical and chemical properties of porphyrins can be controlled by appropriate functionalization of the porphyrin core through post-synthetic modifications [3].

45

Results and discussion

4,4',4'',4'''-(5,10,15,20-porphyrinetetrayl)-tetrabenzoic acid (H_6TCPP) is the most intensively investigated linker for the synthesis of porphyrin-based MOFs. We demonstrated the successful synthesis and characterization of porphyrin-based MOF containing gallium(III) ions i.e., $GaTCPP$ with the chemical composition $[Ga_2(H_2TCPP)(OH)_2] \cdot 5DMF \cdot 2H_2O$ (DMF – *N,N'*-dimethylformamide), which was prepared by hydrothermal synthesis and characterized using a wide range of analytical techniques: infrared spectroscopy, thermogravimetric measurements, elemental analysis and single-crystal structure analysis (SXR). Compound $GaTCPP$ crystallizes in the space group C_{mmm} . The Ga(III) ions are six-coordinated, with the six oxygen atoms originating from the four independent H_2TCPP^{4-} ligands, the remaining two oxygen atoms come from bringing μ -OH groups. Coordination of GaO_6 octahedrons using μ -OH bridges creates a polymer network of trans-corner-sharing polyhedral along the *b* crystallographic axis. Furthermore, the coordination of H_2TCPP^{4-} ligand to eight Ga(III) ions leads to the formation of the final three-dimensional open porous framework containing three mutually crossing pores propagating along all crystallographic. Two

types of cavities are formed each along the *b* and *c* crystallographic axis with the size of approximately $8.1 \times 11.4 \text{ \AA}^2$ and $4.4 \times 8.8 \text{ \AA}^2$, respectively. Infrared spectroscopy confirmed the presence of solvents in cavities and TCPP ligand. The next step of our investigation was the modification process of coordination polymer by its soaking in the DMSO solutions of Ni^{2+} , Co^{2+} . The activated porous complexes were subjected to adsorption measurements of argon at $-186 \text{ }^\circ\text{C}$. Before the surface analysis materials were degassed for 2 hours at $100 \text{ }^\circ\text{C}$ and 16 hours for $140 \text{ }^\circ\text{C}$. Depending on the presence of ion in the structure, we observed the different value of the BET surface area. Fitting of argon adsorption isotherm using the Brunauer–Emmett–Teller (BET) equation gives estimated surface areas (BET) of $1010 \text{ m}^2/\text{g}$, $1187 \text{ m}^2/\text{g}$ and $1188 \text{ m}^2/\text{g}$ for GaTCPP, GaTCPP(Ni^{2+}) and GaTCPP(Co^{2+}), respectively. It is obvious that the post-synthetic modification significantly affected the size of the specific surface area in selected porphyrin-based MOFs. MOFs as a conductive part of cathode material displayed successful sulphur capture and encapsulation proven by stable charge/discharge cycle performances, high-capacity retention, and Coulombic efficiency. The electrodes with pristine GaTCPP showed a discharge capacity of 699 mAh g^{-1} at 0.2 C in the fiftieth cycle. However, the doping of GaTCPP by Ni has a positive impact on the electrochemical properties, the capacity increased to 778 mAh g^{-1} in the fiftieth cycle at 0.2 C .

Acknowledgements

This work was supported by the Scientific Grant Agency of the Slovak Republic (VEGA) under Project 1/0865/21, by the Slovak Research and Development Agency under Contracts APVV-20-0512, APVV-20-138 and, from P. J. Safarik University no. VVGS-2020-1667.

References

- [1] Furukawa, H.; Cordova, K. E.; O’Keeffe, M.; Yaghi, O. M. *Science*, **341** (2013) 1230444.
- [2] Zhou, H.-C.; Long, J. R.; Yaghi, O. M. *Chem. Rev.* **112** (2012) 673–674.
- [3] Gao, W.-Y.; Chrzanowski, M.; Ma, S. *Chem. Soc. Rev.* **43** (2014) 5841–5866.

Boronic Acids and Ferrocenes – from Electroactive Molecular Probes to ROS-activated Prodrugs

M. Konhefr^{a*}, J. Věžník^{a,b}, Z. Fohlerová^c, K. Lacina^b

^a Department of Chemistry, Faculty of Science, Masaryk University, Kamenice 5, 62500 Brno, Czech Republic

^b CEITEC, Masaryk University, Kamenice 5, 62500 Brno, Czech Republic

^c CEITEC, Brno University of Technology, Purkyňova 123, 61200 Brno, Czech Republic

*379848@mail.muni.cz

A chemosensor is a device containing a recognition, a detection, and a transducer unit. It contains small chemical molecules, i.e., molecular probes as signalling elements. The field of (chemo)sensors is already well-developed, especially its part with an optical detection. [1] However, probes possessing an electrochemical detection are still quite scarce. [2]

Hence, our research activities in the field of synthetic and material chemistry started with synthesis, structure elucidation and description of physicochemical properties of derivatives including boronic acids and ferrocenes, especially new aminoferrocene probes. [3] Because an *ortho*-arylboronate has been often employed in enhancing of diol binding [4] which is then effective even at physiological neutral pH, we synthesized and compared three different ((ferrocenylimino)methyl)phenylboronic acids (a, b, c) and their catechol esters, respectively. The further work involved description of their behaviour in electrochemical processes determining functional abilities of the synthesized derivatives using voltammetric techniques and spectroelectrochemistry.

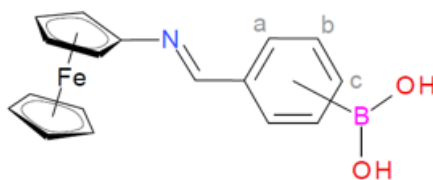


Figure 1: Synthesized ((ferrocenylimino)methyl)phenylboronic acids a, b, c.

The *ortho*-iminoboronate isomer appeared to be an excellent structure for studies of the donor–acceptor properties, (proton-coupled) intramolecular electron transfers and

intramolecular interactions in general. These involve the atomic B–N and B–diol interactions in Lewis's definition. Furthermore, we described electrochemically facilitated reactions on an electron-rich imine bond (redox-controlled, i.e., redox-dependent addition of O-nucleophiles). [5] As a consequence, we also observed complete redox-dependent breakage of imine bond in non-aqueous solvent in the presence of NaCl facilitated by electrochemical cycling of the *ortho*-iminoboronate. [6]

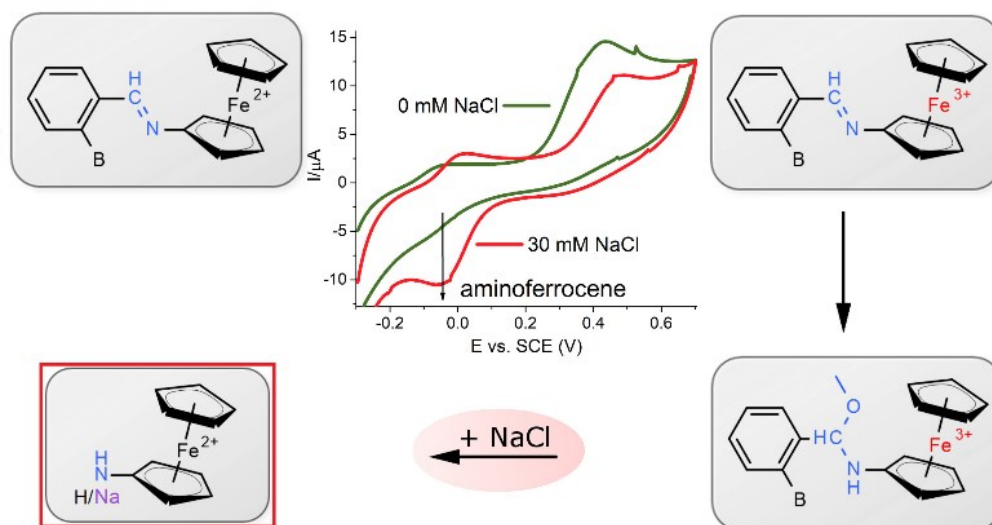


Figure 2: Redox-dependent breakage of imine bond in non-aqueous solvent in the presence of NaCl facilitated by electrochemical cycling of the *ortho*-iminoboronate derivative.

Current possibilities of utilization of electroactive boronic acids lay not only in a molecular recognition (analytical sensing) but also in drug development (drug delivery and on-demand release). Such a functional material arisen from this research field can be applied as an enzyme inhibitor or an advanced boronic acid-based smart material with properties of stimuli-responsiveness. The reactive oxygen species (ROS), pH or diols can serve as a stimulus for a coupled functional task. At last, but not least, also ferroptosis and biochemical processes leading to e.g., anticancer activity which deal with elevated or suppressed levels of ROS and pH in cells, can be influenced by these electroactive boronic acids as (pro)drugs. [7] First trials examining cytotoxic abilities of the iminoboronates have been currently done in which *para*-iminoboronate catechol ester showed slightly higher cytotoxicity than aminoferrocene as a control. [8]

Acknowledgements

This research has been financially supported by the Ministry of Education, Youth and Sports of the Czech Republic under the project CEITEC 2020 (LQ1601), by Masaryk University under the project (MUNI/A/1424/2019), and by the Czech Science Foundation, grant nr. 19-16273Y. We also acknowledge CF Nanobiotechnology supported by MEYS CR (LM2015043) and CEITEC Nano+ project CZ.02.1.01/0.0/0.0/ 16_013/0001728.

References

- [1] You, Zha and Anslyn, *Chemical Reviews*, **2015**, 115, 7840–7892.
- [2] Anzai, *Materials Science and Engineering: C*, **2016**, 67, 737–746.
- [3] Konhefr, Lacina et al., *Monatshefte für Chemie – Chemical Monthly*, **2017**, 148, 11, 1953–1958.
- [4] James, Phillips and Shinkai, *Boronic acids in saccharide recognition*, Stoddart (Ed.), RSC, **2006**.
- [5] Konhefr, Lacina et al., *ChemistrySelect*, **2018**, 3, 33, 9641–9647.
- [6] Konhefr, Michalcová et al., *Tetrahedron Letters*, **2020**, 61, 151535.
- [7] Daum, Mokhir et al., *Bioconjugate Chemistry*, **2019**, 30, 1077–1086.
- [8] Věžník, Konhefr et al., *Journal of Inorganic Biochemistry*, **2021**, 224, 111561.

Microscopic Simulation of Li-ion Battery

M. Mačák^{a*}, P. Vyroubal^a and T. Kazda^a

^a Department of Electrical and Electronic Technology, Brno University of Technology,
Brno 616 00, Czech Republic

*Email address: martin.macak@vut.cz

Introduction

Li-ion batteries are one of the most important storage systems as they play an important role in the smart grid and electrified vehicle applications. Even though this technology is generally well established, there are still many challenges, which inhibit a widespread application of electric vehicles [1, 2]. One of the main researched areas is the improvement of charging process without accelerating degradation of batteries. The other area is the battery safety, which can be compromised by external or internal forces [3]. Both areas are based on the changes in the battery microstructure [2, 3]. Experimental investigation of these processes is often complicated and time consuming as it is necessary to age the battery and then to study the degradation, usually by complex visualization methods [3].

Numerical simulations pose as a suitable alternative as they can describe relevant processes at different length scales. Most approaches describe Li-ion batteries from a macroscopic point of view, which requires a simplification of the geometry as well as of the physics description [4, 5]. To precisely study electrochemical and mechanical processes inside a battery, it is necessary to resolve a detailed geometry of the structure [6, 7, 8]. Then these results can be used as a basis for simplified macroscopic models.

This article presents a microscopic simulation of a Li-ion battery carried out in Ansys Fluent. The simulations focused on the influence of the electrode structure on the electrochemical processes. The possibility of extending the model to include mechanical stresses caused by volume change and the effects of side reactions was also studied.

Numerical Model

The microscopic model of a Li-ion battery presented in this work is based on the direct resolution of lithium transport in the electrolyte and the electrode phase [7, 8]. The transport of lithium ions inside electrode particles is governed by a simple diffusion equation. Migration of lithium ions in the electrolyte is based on concentrated solution theory, which includes both solute-solvent and solute-solute interactions [7]. The

chemistry of charge transfer reactions occurs at the solid-electrolyte interface and is described by the Butler-Volmer equation, which also includes the effects of concentration limitation [8]. Similarly to species transport, the charge conservation is also solved separately in the electrode and the electrolyte regions. This separation of electric potential leads to a simplified definition of the electric field, in which it is not necessary to solve double layer at the particle surface.

The simplified geometry of a Li-ion battery structure used in simulations consisted of three areas: cathode particle, electrolyte, and anode particles. Particle properties and reaction parameters were obtained from [8].

Discussion

Simulations showed that it is possible to use the presented model for microscopic modelling of Li-ion electrochemistry. The critical point of simulations lied in the proper definition of material and reaction parameters and especially the definition of equilibrium potential. Generally, all Li-ion batteries are governed by intercalation and deintercalation mechanism, so the equilibrium potential is the main factor, which describes the exact battery chemistry. The advantage of this model is that it was possible to study the effects of particle size distribution on the behavior of Li-ion batteries. Based on these simulations, it might be possible to estimate the optimal particle size distribution and total thickness of the electrodes. It was shown that increasing the size of individual particles as well as the overall size of the electrodes will inhibit lithium transport, which will in result slow the electrochemical reaction.

Currently, the presented model is purely focused on electrochemical processes. The mechanical stresses and deformation can be included using dynamic mesh module or by coupling Ansys Fluent with Ansys Mechanical software. This way, it would be possible to study effects of particle volume change and subsequent cracking. The effects of parasitic or side reactions might be included by implementing custom function to describe reaction kinetics and material parameters.

Acknowledgements

This work was supported by the BUT specific research program (project No. FEKT-S-20-6206).

References

- [1] L. Li, Y. Ren, K. O'Regan, U. R. Koleti, E. Kendrick, W. D. Widanage, and J. Marco, *Journal of Energy Storage*. **44**, 103324 (2021).
- [2] A. Jnawali, A. N. P. Radhakrishnan, M. D. R. Kok, F. Iacoviello, D. J. L. Brett, and P. R. Shearing, *Journal of Power Sources*. **527**, 231150 (2022).
- [3] L. K. Willenberg, P. Dechent, G. Fuchs, D. U. Sauer, and E. Figgemeier. *Sustainability*, **12** (2), (2020).
- [4] C. Lin and A. Tang, *Energy Procedia*. **104**, 68-73 (2016).
- [5] A. Nikolian, J. Jaguemont, J. de Hoog, S. Goutam, N. Omar, P. Van Den Bossche, and J. Van Mierlo, *International Journal of Electrical Power & Energy Systems*. **98**, 133-146 (2018).
- [6] A. M. Boyce, E. Martínez-Pañeda, A. Wade, Y. S. Zhang, J. J. Bailey, T. M. M. Heenan, D. J. L. Brett, and P. R. Shearing, *Journal of Power Sources*. **526**, 231119 (2022).
- [7] G. M. Goldin, A. M. Colclasure, A. H. Wiedemann, and R. J. Kee. *Electrochimica Acta*, **64**, 118-129 (2012).
- [8] A. M. Colclasure and R. J. Kee. *Electrochimica Acta*, **55**(28), 8960-8973 (2010).

Activated carbon as a conductive host in Li-S battery

V. Niščáková^{a*}, A. Straková Fedorková^a

^a Department of Physical Chemistry, Faculty of Science, P. J. Šafárik University in Košice, Moyzesova 11, 041 54, Košice

*veronika.niscakova@student.upjs.sk

In today's modern society, energy is an increasingly important part of life, from everyday needs to modern technology. With the ever-increasing demand for sustainable energy, an energy resource should be based more on non-fossil sources, and this resource should be affordable, environmentally friendly, and inexhaustible [1].

The development of batteries as a fast source of energy has increased significantly since the beginning of the commercialization of Li-ion batteries (LiB). Despite their widespread use in diverse devices and technologies, LiBs have various limitations that researchers are trying to improve, and their aim is to develop a better power source that exceeds LiB's performance [2]. Li-S batteries are due to their efficient properties have gained attention as promising candidates for the next-generation energy storage applications. Li-S batteries have up to five times greater energy density than LiBs (about 2600 W h kg⁻¹) and their standard open-circuit potential of 2,15 V [2,3].

The cathode is a significant component of every battery but this component brings serious problems which researchers examine and test and try to improve it. Sulphur is usually combined and improved with a substrate with high electronic conductivity since sulphure has low conductivity. Most often used material for improve conductivity of cathode is carbon material [1,3].

In this work, was prepared a positive electorde for a Li-S battery. Composition of this cathode was 80% sulphur; 10% activated carbon, and 10% PVDF (polyvinylidene fluoride as a binder). The prepared electrode was tested by electrochemical procedures such as cyclic voltammetry and galvanostatic cycling. The cycling took place in the range of potentials from 1,8 V – 2,8 V. The initial discharge capacity at 0.1 C was 230 mAh/g. Prepared electrode was than cycling at 0,2 C for 20 cycles and capacity after first cycle was 406,82 mAh/g, and after 20 cycles capacity decreased to 286,25 mAh/g.

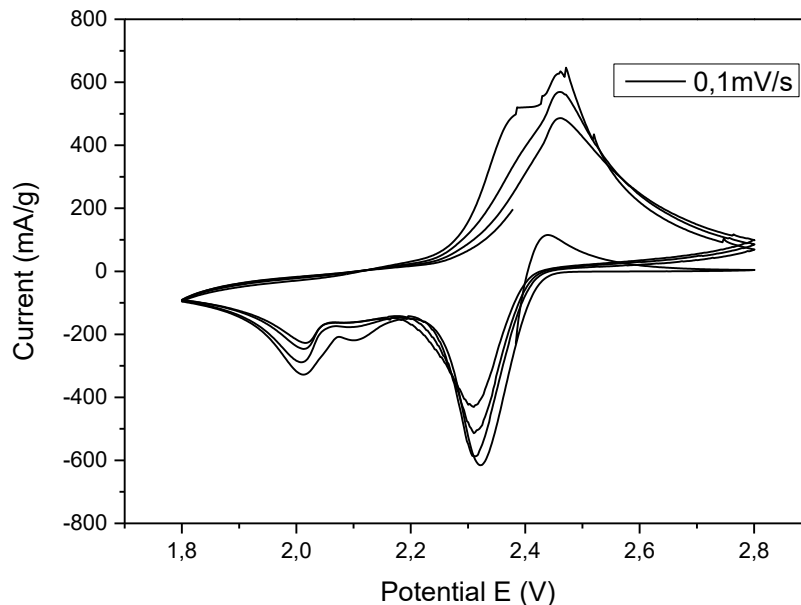


Figure 6: CV curves of S – AC as a scan rate of 0.1 mV/s.

Acknowledgements

This publication was supported by the Operational program Integrated Infrastructure within the project: Innovative Solutions for Propulsion, Power and Safety Components of Transport Vehicles, 313011V334, cofinanced by the European Regional Development Fund and of the Slovak Research and Development Agency APVV-20-0138 and APVV-20-0111.

References

- [1] Z. Gao, Y. Zhang, N. Song, X. Li, Biomass-derived renewable carbon materials for electrochemical energy storage, *Mater. Res. Lett.* **5** (2017) 69–88.
- [2] C. McCreary, Y. An, S.U. Kim, Y. Hwa, A perspective on li/s battery design: Modeling and development approaches, *Batteries.* **7** (2021) 1–24.
- [3] Y.X. Yin, S. Xin, Y.G. Guo, L.J. Wan, Lithium-sulfur batteries: Electrochemistry, materials, and prospects, *Angew. Chemie - Int. Ed.* **52** (2013) 13186–13200.

Nickel nanocavity prepared by colloidal lithography as a suitable electrochemical sensor for insuline detection

O.Petruš^{a*}, I.Šišoláková^b, R. Oriňaková^b

^a Institute of Materials Research, Slovak Academy of Sciences,
Watsonova 47, 040 01 Košice

^b Department of Physical Chemistry, Pavol Jozef Šafárik University in Košice,
Moyzesova 11, 040 01, Košice

*opetrus@saske.sk

Considering the growing prevalence of diabetes mellitus, an electrochemical sensor for the determination of insulin was proposed for the effective diagnosis of the disease. Colloidal lithography in combination of electrochemical deposition is suitable method to prepare highly ordered nanostructures with large area as you can see on Fig 1° [1]. The prepared Ni nanocavities ensured the considerable expansion of the active surface area in comparison to bare unmodified conductive glass or conductive glass modified by an even Ni layer. The average diameter of the nanocavities calculated to be 498 ± 38 nm and the diameter distribution histogram can be seen on Fig 1B.

55

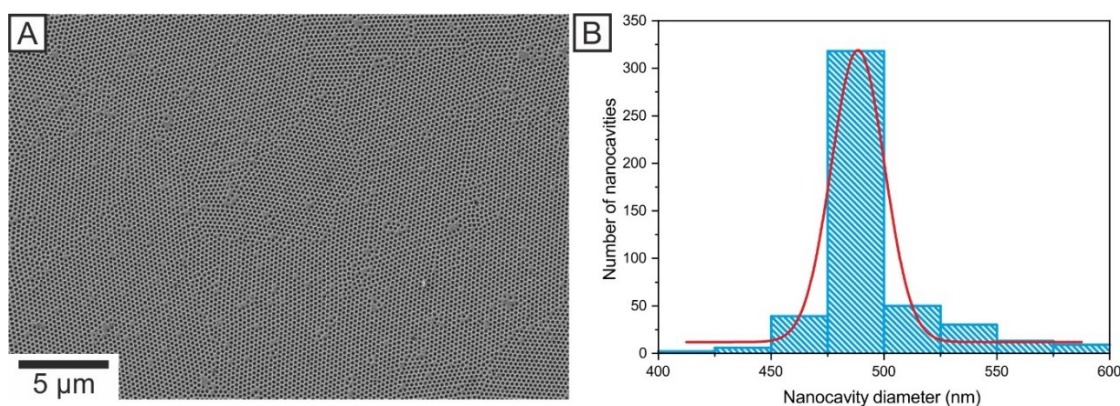


Figure 7: SEM image of Ni nanoparticles modified carbon electrode.

The insulin assay performance was evaluated by cyclic voltammetry. Ni-c-ITO exhibited excellent analytical characteristics, including high sensitivity ($1.032 \mu\text{A } \mu\text{mol}^{-1} \text{dm}^3$), a low detection limit ($156 \mu\text{mol dm}^{-3}$), and a wide dynamic range (500 nmol dm^{-3} to $10 \mu\text{mol dm}^{-3}$). In addition, the stability of the Ni-c-ITO electrodes is over 50 measurements, which is shown in Fig 2A,B. CV in $\text{K}_3[\text{Fe}(\text{CN})_6]/\text{K}_4[\text{Fe}(\text{CN})_6]$ suggests that there is no reduction in

electroactive area even after repeated measurements. This is also confirmed by the measurement of 2×10^{-6} mol dm⁻³ insulin in 0.1 mol dm⁻³ NaOH and PBS, where the measured current decrease only by ~ 8 %. Importantly, Ni-c-ITO acted as a selective sensor for the detection of insulin in blood serum, enabling its future applications in clinical diagnosis.

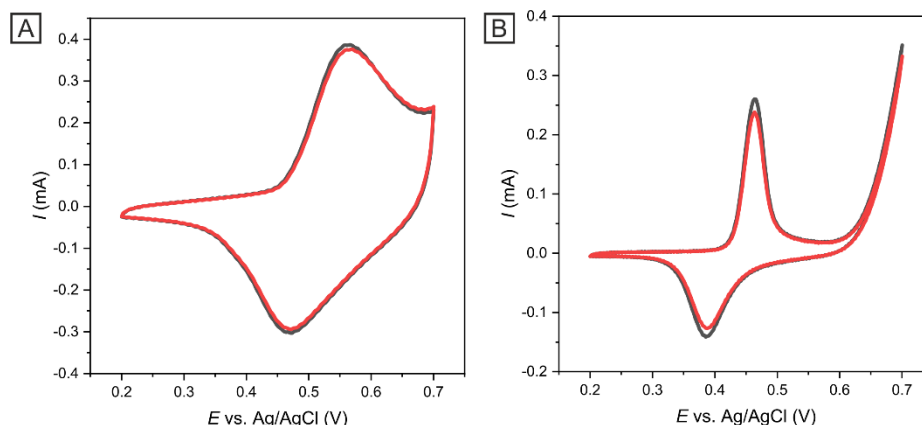


Figure 8: CV measurements used for the evaluation of the stability of Ni-c-ITO using 1×10^{-3} mol dm⁻³ $K_3[Fe(CN)_6]/K_4[Fe(CN)_6]$ in 1 mol dm⁻³ KCl at 50 mV s^{-1} (A) and 2×10^{-6} mol dm⁻³ insulin in 0.1 mol dm⁻³ NaOH and PBS (B). Black line (1st measurement) and red line (50th measurement).

Acknowledgments

This research work has been supported by the Research Agency of the Ministry of Education, Science, Research and Sport of the Slovak Republic, by the project: Advancement and support of R&D for “Centre for diagnostics and quality testing of materials” in the domains of the RIS3 SK specialization, Acronym: CEDITEK II., ITMS2014+ code 313011W442, “R

esearch Centre of Advanced Materials and Technologies for Recent and Future Applications” “PROMATECH” ITMS: 26220220186, APVV-PP-COVID-20-0036 and APVV-20-0278 of the Slovak Research and Development Agency, and Visegrad Fund project number 22020140.

References

[1] O. Petruš, A. Oriňak, R. Oriňaková, Z. Orságová Králová, E. Múdra, M. Kupková, K. Koval', Appl. Surf. Sci. **423** (2017) 322-330

Metal-organic frameworks containing fluorinated ligands

Dávid Princík^{a*}, Vladimír Zeleňák^a.

^a Department of Inorganic Chemistry, Faculty of Science, P. J. Šafárik University,
Moyzesova 11, 041 54 Košice, Slovak Republic

* david.princik@student.upjs.sk

The last two decades have received a huge expansion in the field of crystal polymeric porous materials also known as Metal-Organic Frameworks (MOF). These versatile materials dominate mainly due to their surface area and pore volume with various pore topologies, accessible cages and their potential applications in different fields, such as heterogenous catalysis [1], gas storage and gas separation materials [2] or drug delivery systems. Despite their great advantages, these materials also have certain disadvantages. From an industrial point of view, the main disadvantage is the hydrolytic lability, which is compensated by drying the used reactants, gases or solvents, which increases the production costs. Several methods are known to increase the hydrolytic resistance of MOF materials, but they often lead to pore occupancy and potentially decrease the sorption capacity of gases [3].

In this work we focus on increasing the hydrolytic resistance of MOF-type materials using a synthetic method that includes a completely new synthesis of MOF materials from a series of new, hydrophobic fluorinated ligands. Their hydrophobic effect is ensured by the aromatic skeleton of the ligand and the fluorine atoms bound to it. Two series of MOF complexes with non-fluorinated ligand as a reference material and fluorinated derivative were prepared. The first ligand represents biphenyl-4,4'-dicarboxylic acid (H₂BPDC), with which MOF complexes have been successfully prepared using Zn²⁺, Ba²⁺, Ce³⁺, Fe³⁺, Cr³⁺, La³⁺, Yb³⁺ and Zr⁴⁺ salts. The second ligand represents 3,3',5,5'-tetrafluorobiphenyl-4,4'-dicarboxylic acid (H₂4FBPDC), with which MOF complexes have been prepared using Ba²⁺, Ce³⁺, Cr³⁺ and La³⁺ salts and all prepared MOF complexes were subjected to IR, TG and SXRD measurements confirming their composition. Experimental results confirm the increased stability of fluorinated derivatives compared to reference complexes. Detailed information will be presented at the conference. Communications regarding the conference will be sent to the corresponding author.

Acknowledgements

This work was supported by the Scientific Grant Agency (VEGA 1/0865/21).

References

- [1] S. Li, Y. Zhang, Y. Hu, B. Wang et al., J. Materiomics. **7** (2021) 1029-1038.
[2] Q.-F. Qiu, C.-X. Chen, Z. Zeng et al., Inorg. Chem. **59** (2020) 14856-14860.
[3] S.-Y. Jiang, W.-W. He, S.-L Li. et al., Inorg. Chem. **57** (2018) 6118-6123.

Electrochemical Determination of Insulin

I.Šišoláková^{a*}, O. Petruš^b, J. Shepa^a, R. Oriňaková^a

^a Department of Physical Chemistry, Pavol Jozef Šafárik University in Košice,
Moyzesova 11, 040 01, Košice

*ivana.sisolakova@upjs.sk

Electrochemical sensors can be considered as the novel tool for fast, occurrence, and low-cost diseases diagnostics. Various worldwide serious diseases such as diabetes mellitus, various types of cancer, Parkinson's disease, Alzheimer's, viruses' diseases can be diagnostic via electrochemical methods [1]. Our previous work has focused on developing suitable electrochemical sensors for diabetes mellitus, epidermal growth factor receptor (EGFR), and various viruses' disease diagnostics (COVID 19). Since diabetes mellitus can be considered one of the most widespread diseases worldwide, a fast and cheap diagnosis is desirable. In our research, various type of carbon electrodes modification for insulin determination has been studied. Various metals such as Ni, Cu, Zn, and Co were tested. Based on our research the most suitable modification material for electrochemical insulin determination Ni was chosen. The huge disadvantage of Ni nanoparticles modified carbon electrodes arising from alkaline pH which was necessary for electrochemical measurement because of the catalytic particle NiOOH^- originating only in alkaline medium. Therefore, we decided to develop electrochemical sensor modified via Ni nanoparticles for insulin determination in neutral pH. First, the SEM images with EDX analysis of Ni modified carbon electrodes were obtained, where the 16,2% of Ni was confirmed.

59

After that special activation method via 0.1 M NaOH was applied and insulin was determined on this activated electrode in various pH (alkali, neutral, and acidic). As can be seen in Figure 2, both alkaline and neutral pH was suitable for further insulin determination with the compared current response. The current response towards insulin oxidation was 0.0081 μA , and 0.0075 μA for alkaline, and neutral pH, respectively. Based on these results we can conclude that Ni nanoparticles modified carbon electrodes activated in accurate procedure in 0.1 M NaOH can be considered as the suitable electrochemical sensor for insulin determination in neutral pH.

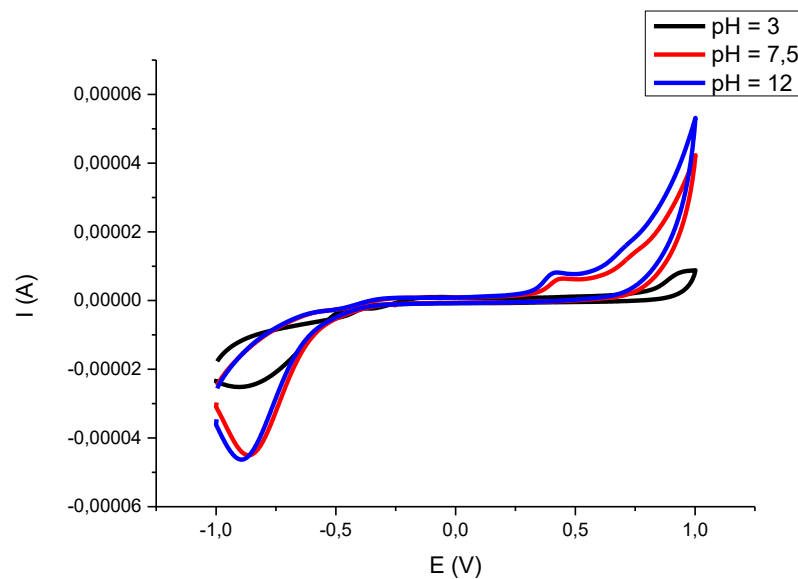


Figure 1: Cyclic voltammograms of 2 μM insulin in various pH.

Acknowledgments

This work has been supported by the project of the Slovak Research and Development Agency APVV-PP-COVID-20-0036 and Visegradfund project number 22020140.

60

References

[1] L. C. Martinez, D. Sherling, A. Holley, *Prim. Care - Clin. Off. Pract.* **46** (2019) 41–52.

SBA-15 coated with nanocrystalline NiO-doped anatase as heterogeneous catalyst for photodegradation of organic molecules

L. Zauška^{a*}, M. Almáši^a

^a Department of Inorganic Chemistry, Faculty of Science, P. J. Šafárik University,
Moyzesova 11, SK-041 01 Košice, Slovakia

*l.zauska@gmail.com

Water is an essential part of our life. It is necessary for life being, biological and biochemical processes in the nature and human body. In decades, due to industry, water ecology was decreased significantly. In rural parts of European countries, agriculture contaminated water with pesticides and their metabolic products. And so contaminated water is a source of drinking water for mentioned rural areas. Due to high prices, a large percentage of the population has no water purification system. Also, some countries report increased medicaments and hormones in wastewater and drinkwater [1]. In both cases, the concentrations of mentioned organic pollutants are low and do not represent high-risk illnesses in the short term. In the long term, these pollutants have a high risk of occurrence cancer, liver and kidneys damage, and gastrointestinal problems.

The water purification technologies are expensive, service cost is too high, and filtration media can not be reusable or recycled. The second majority problem is the toxicity of mentioned used media. But there are some methods for how pollutants like heavy metal ions and organic compounds can be removed from wastewater without back elution from sorbent after filling it: The way is the ecologic oxidation of organic waste. The oxidation must be established on physicochemical reactions like photocatalysis [2]. Photocatalytic oxidation of organic pollutants and pathogens occurs on nanomaterials like TiO₂, ZnO₂ and BiVO₄. The photocatalytic effect arises during electron transfer from valence bands through the bandgap to the conduction band. This electron must be excited with high energy photons in the UV – VIS light range. Material doping with any atoms has a possibility to reduce the required energy for electron transfer, and this way raises catalyst effectivity.

Prepared material NiO@TiO₂@SBA-15 was characterised via several analytical methods: Nitrogen adsorption was realised at 77K in pressure range of $p/p_0 = 0.05 - 0.95$ on APAP 2020 from Micromeritics Co. Surface area was determined with Brunauer-Emmett-Teller (BET) mathematical model. UV-VIS spectroscopy was used to characterise the photocatalyst effectivity and degradation of organic compounds were determined in the range of 200-380 nm. The mesoporous silica's texture properties and morphology were checked with the transmission electron microscopy and energy-dispersive spectroscopy (TEM and EDS) on JEM 2100F UHR, from Jeol Co.

As shown from Fig. 1, TEM confirmed the presence of nanocrystalline anatase (TiO₂) on the SBA-15 surface. Moreover, EDX analysis confirmed the presence of NiO and the elemental map of SiO₂, TiO₂ and NiO is also shown in Fig. 1.

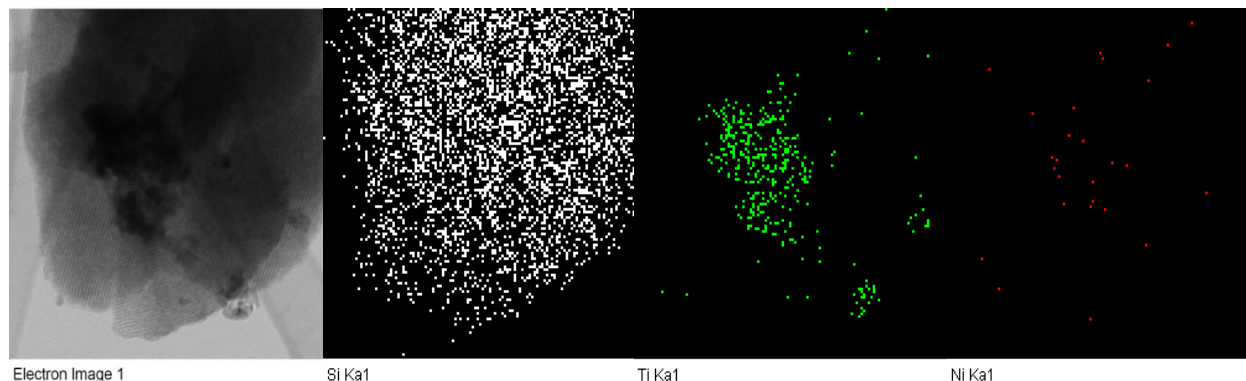


Figure 9: TEM images of NiO@TiO₂@SBA-15 composite.

First, the material was tested on methylene blue and methyl orange for photoactivity, where decolouration of selected pigments was observed. These testing experiments were realised with UV-A light at 365 nm and 100 mg photoactive material. In the case of methylene blue, the color of mixture was changed from blue to grey, and after filtration, the filtrate was clear without the presence of dye (see Fig. 2). In the case of methyl orange, the colour solution after catalytic decomposition was light yellow.

In conclusion, this novel composite material shows a tremendous photocatalytic effect. Due to its relatively high surface area (aprox. 250 m² based on nitrogen adsorption), it has excellent filtration properties for effective organic waste capture its ecological degradation.

62

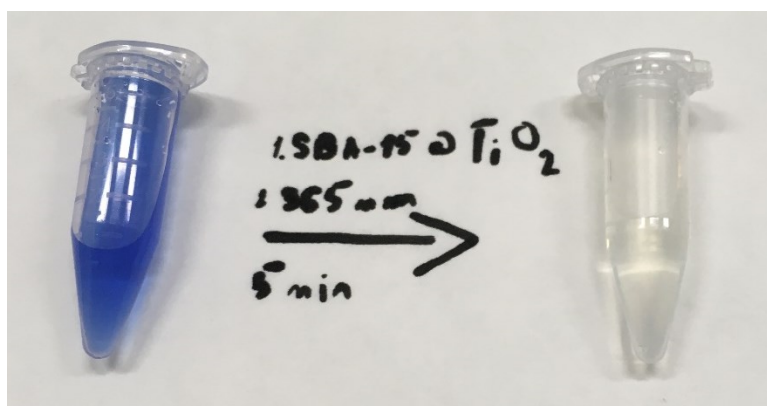


Figure 10: Methylene blue photodegradation.

Acknowledgements

This work was supported by the project VVGS-PF-2021-2092.

References

[1] Al-Ahmad, A. et. al., Spring. **37** (1999) 158.

[2] Park, H., et. al., J. Photochem. Photobiol. C: Photochem. Rev. **15** (2013) 1.

Spring electrochemical Meeting

Book of Abstracts

Edited by: RNDr. Ivana Šišoláková, PhD.

Publisher: Pavol Jozef Šafárik University in Košice
Publishing ŠafárikPress

Year: 2022

Pages: 66

Author's sheets: 2,4

Edition: first

ISBN 978-80-574-0089-9 (e-publikation)